Europe PMC Funders Group
Author Manuscript
Sci Immunol. Author manuscript; available in PMC 2024 January 05.

Published in final edited form as:
Sci Immunol. 2023 December 15; 8(90): eabo5558. doi:10.1126/sciimmunol.abo5558.

Acquisition of suppressive function by conventional T cells limits anti-tumor immunity upon T_{reg} depletion

Sarah K. Whiteside[1], **Francis M. Grant**[2], **Giorgia Alvisi**[3], **James Clarke**[4], **Leqi Tang**[1], **Charlotte J. Imianowski**[1], **Baojie Zhang**[1], **Alexander C. Evans**[1], **Alexander J. Wesolowski**[1], **Alberto G. Conti**[1], **Jie Yang**[1], **Sarah N. Lauder**[5], **Mathew Clement**[5], **Ian R. Humphreys**[5], **James Dooley**[1], **Oliver Burton**[1], **Adrian Liston**[1], **Marco Alloisio**[6,7], **Emanuele Voulaz**[6,7], **Jean Langhorne**[8], **Klaus Okkenhaug**[1], **Enrico Lugli**[3], **Rahul Roychoudhuri**[1]

[1]Department of Pathology, University of Cambridge, Tennis Court Road, CB2 1QP, UK

[2]Immunology Programme, Babraham Institute, Babraham Research Campus, Cambridge, Cambridgeshire, CB22 3AT, UK

[3]Laboratory of Translational Immunology, IRCCS Humanitas Research Hospital, Via Manzoni 56, 20089 Rozzano – Milan, Italy

[4]La Jolla Institute for Allergy and Immunology, La Jolla, CA

[5]Division of Infection and Immunity/System Immunity University Research Institute, Cardiff University, Cardiff CF14 4XN, UK

[6]Department of Biomedical Sciences, Humanitas University, Via Rita Levi Montalcini 4, 20072 Pieve Emanuele – Milan, Italy

[7]Division of Thoracic Surgery, IRCCS Humanitas Research Hospital, Via Manzoni 56, 20089 Rozzano – Milan, Italy

[8]The Francis Crick Institute, 1 Midland Road, London NW1 1AT

Abstract

Regulatory T (T_{reg}) cells contribute to immune homeostasis but suppress immune responses to cancer. Strategies to disrupt T_{reg} cell-mediated cancer immunosuppression have been met with limited clinical success, but the underlying mechanisms for this failure are poorly understood. By

This work is licensed under a BY 4.0 International license.

Correspondence to: Sarah K. Whiteside; Rahul Roychoudhuri.

Correspondence should be addressed to S.K.W. (sw925@cam.ac.uk) and R.R. (rr257@cam.ac.uk).

Author contributions

S.K.W. and R.R. conceived and designed experiments; S.K.W., F.M.G., G.A., J.C., L.T., C.J.I., B.Z., A.C.E., A.C., A.W., S.N.L., M.C., J.D. conducted experiments, S.K.W., G.A., J.C., A.C.E., E.L., and R.R. performed analyses and data visualization. S.K.W., I.H.R., E.L., and R.R. provided funding; S.K.W. O.B., J.C., J.Y., I.R.H., J.L., K.O., and R.R., developed the methodology used; S.K.W., O.B., A.L., E.L., and R.R. provided supervision; M.A., E.V., G.A., and E.L., coordinated and obtained he clinical samples, S.K.W. and R.R wrote the original draft, S.K.W., C.J.I., E.L., and R.R. reviewed and edited the paper.

Competing interests

R.R. holds or has held paid consultancies with Lyell Immunopharma, Achilles Therapeutics and Enhanc3D Genomics; and is a principal investigator of research projects funded by AstraZeneca and F-star Therapeutics on unrelated topics that do not constitute competing interests. E.L. served as a consltant for BD Biosciences on a topic unrelated to this work. All other authors declare no competing interests.

Europe PMC Funders Author Manuscripts
Europe PMC Funders Author Manuscripts

Europe PMC Funders Author Manuscripts

Europe PMC Funders Author Manuscripts

modeling T_{reg} cell-targeted immunotherapy in mice, we find that $CD4^+$ $Foxp3^-$ conventional T (T_{conv}) cells acquire suppressive function upon depletion of $Foxp3^+$ T_{reg} cells, limiting therapeutic efficacy. $Foxp3^-$ T_{conv} cells within tumors adopt a T_{reg} cell-like transcriptional profile upon ablation of T_{reg} cells and have a similar capacity to suppress T cell activation and proliferation *ex vivo*. Suppressive activity is enriched among $CD4^+$ T_{conv} cells marked by expression of C-C motif receptor 8 (CCR8), which are found in mouse and human tumors. Upon T_{reg} cell depletion, $CCR8^+$ T_{conv} cells undergo systemic and intratumoral activation and expansion, and mediate IL-10 dependent suppression of anti-tumor immunity. Consequently, conditional deletion of *Il10* within T cells augments anti-tumor immunity upon T_{reg} cell-depletion in mice, and antibody blockade of IL-10 signaling synergizes with T_{reg} cell depletion to overcome treatment resistance. These findings reveal a secondary layer of immunosuppression by T_{conv} cells released upon therapeutic T_{reg} cell depletion and suggest that broader consideration of suppressive function within the T cell lineage is required for development of effective T_{reg} cell-targeted therapies.

Introduction

Immune checkpoint blockade therapies targeting the inhibitory receptors PD-1 and CTLA-4 on T_{conv} cells have revolutionized the treatment of advanced cancer (1–5). However, only a minority of patients with a subset of cancers respond to existing therapies (6–8), necessitating development of mechanistically distinct modes of immunotherapy. T_{reg} cells play a critical role in suppressing endogenous and immunotherapy-driven anti-tumor immunity (9–14). High relative ratios of T_{reg} cells to $CD4^+$ or $CD8^+$ T_{conv} cells within tumors are associated with poor prognoses in patients with a variety of cancers, including ovarian cancer (15, 16), breast cancer (17), non-small cell lung carcinoma (18), hepatocellular carcinoma (19), renal cell carcinoma (20), pancreatic cancer (21), gastric cancer (22), cervical cancer (23), intrahepatic cholangiocarcinoma (24) and colorectal carcinoma (25). $Foxp3^+$ T_{reg} cells also powerfully contribute to immunotherapy resistance, including to immune checkpoint inhibitor therapy (18, 26–28). There is intense medical interest in therapeutically depleting T_{reg} cells or modulating their immunosuppressive function in cancer patients.

Despite abundant experimental evidence of the immunosuppressive role of T_{reg} cells in cancer, T_{reg} cell-targeted therapies have had limited success in the clinic. Agents developed for depletion of T_{reg} cells in humans have included daclizumab (Zenapax), a monoclonal antibody against CD25 which is expressed highly on the surface of most T_{reg} cells, denikeukin difitox (Ontak), an IL-2:diphtheria toxin fusion protein that targets T_{reg} cells through their ability to bind IL-2, and mogamulizumab, a depleting monoclonal antibody against CCR4, which is expressed by high frequencies of tumor-infiltrating T_{reg} cells (29). Daclizumab therapy failed to enhance the efficacy of a dendritic cell vaccine in metastatic melanoma patients (30), and only modestly increased immune response parameters in patients with glioblastoma (31) and breast cancer (32), while denikeukin difitox treatment failed to induce clinical responses in metastatic melanoma patients (33). Mogamulizumab therapy lacked anti-tumor efficacy in advanced cancer patients (34), likely attributable to concomitant depletion of activated $CD4^+$ and $CD8^+$ T_{conv} cells expressing CCR4 (35). Lack

Europe PMC Funders Author Manuscripts

Europe PMC Funders Author Manuscripts

of clinical efficacy despite depletion of T_{reg} cells in many cases indicates a need to discern the basis for treatment failure of T_{reg} cell-targeted therapies.

In this study, we sought to better understand mechanisms of treatment failure of T_{reg} cell-targeting cancer immunotherapies. We systematically evaluated the consequence of experimental T_{reg} cell ablation on T_{conv} cells within tumors. Whereas $CD4^+$ and $CD8^+$ T_{conv} cells were markedly transcriptionally distinct from T_{reg} cells under steady-state conditions, T_{reg} cell ablation caused T_{conv} cells to adopt a T_{reg} cell-like transcriptional profile, upregulating expression of molecules associated with T_{reg} cell suppressive function. Consistent with acquisition of a T_{reg} cell-like transcriptional profile, $Foxp3^-$ T_{conv} cells from T_{reg} cell-depleted animals acquired a potent ability to suppress T_{conv} activation and proliferation *in vitro*, attributable to the expansion and activation of a subset of T_{conv} cells marked by expression of CCR8. This subset of suppressive T_{conv} cells was found to be enriched in both murine and human tumors, and its suppressive function was dependent upon IL-10. Consequently, conditional deletion of *Il10* specifically within T cells, and blockade of IL-10 receptor (IL-10R) signaling during T_{reg} cell depleting immunotherapy reversed treatment failure and resulted in enhanced tumor clearance. These findings indicate that compensatory suppression by T_{conv} cells limits efficacy of T_{reg} cell-targeted therapeutic depletion and suggests that broader consideration of suppressive activity within the T cell lineage will be required for development of more effective therapies.

Results

T_{reg} cell ablation causes T_{conv} cells to adopt a T_{reg} cell-like transcriptional profile

T_{reg} cell depletion has had limited success in cancer patients with advanced disease. To better understand mechanisms underlying treatment failure in the context of therapeutic T_{reg} cell ablation, we utilized *Foxp3*$^{EGFP\text{-}DTR}$ mice, which express human diphtheria toxin receptor (DTR) and enhanced green fluorescent protein (EGFP) under the transcriptional control of the endogenous *Foxp3* gene. Administration of diphtheria toxin (DTx) to *Foxp3*$^{EGFP\text{-}DTR}$ mice enables selective depletion of $Foxp3^+$ T_{reg} cells (36). We subcutaneously implanted syngeneic B16-F10 melanoma cells into *Foxp3*$^{EGFP\text{-}DTR}$ mice and ablated T_{reg} cells through administration of DTx. Early T_{reg} cell ablation (before tumors were palpable) resulted in incomplete rejection of primary tumors, whereas T_{reg} cell depletion in mice with established tumors had little discernible effect upon tumor growth (Fig. 1A), despite near complete ablation of Foxp3-expressing T_{reg} cells within the systemic and intratumoral compartments of DTx-treated mice (Fig. 1B).

To understand mechanisms of treatment resistance, we first examined the consequence of T_{reg} cell ablation on the transcriptional profiles of $CD4^+$ and $CD8^+$ T_{conv} cells within tumors. Surprisingly, although intratumoral *Foxp3*$^{EGFP-}$ $CD4^+$ and $CD8^+$ T_{conv} cells were markedly transcriptionally distinct from *Foxp3*$^{EGFP+}$ T_{reg} cells under steady-state conditions, T_{reg} cell depletion caused *Foxp3*$^{EGFP-}$ T_{conv} cells to adopt a T_{reg} cell-like transcriptional profile. We noted that a large proportion of genes specifically enriched within tumor-associated T_{reg} cells compared with $CD4^+$ T_{conv} cells ($|FC| > 4$, $q < 0.05$) under steady-state conditions were induced at high levels within $CD4^+$ or $CD8^+$ T_{conv} cells upon T_{reg} cell ablation (Fig. 1C and 1D; Data file S1). Clusters A and B comprised intratumoral

Europe PMC Funders Author Manuscripts

Europe PMC Funders Author Manuscripts

T_{reg} cell-associated genes upregulated in both $CD4^+$ and $CD8^+$ T_{conv} cells upon T_{reg} cell ablation; Cluster C contained intratumoral T_{reg} cell-associated genes whose expression was upregulated exclusively in $CD8^+$ T_{conv} cells; Cluster D included intratumoral T_{reg} cell-associated genes whose expression was upregulated exclusively in $CD4^+$ T_{conv} cells; Cluster E comprised a limited set of T_{reg} cell-specific transcripts that were not expressed at high relative levels in $CD4^+$ or $CD8^+$ T_{conv} cells, including *Foxp3, Lrrc32, Ikzf2, Runx2*, and *Ctla4*. Similarly, a substantial fraction of transcripts highly expressed within intratumoral T_{conv} cells compared with T_{reg} cells were downregulated within T_{conv} cells upon T_{reg} cell ablation. (Fig. S1; Data file S2). Consistent with these observations, hierarchical clustering analysis of Pearson distances between global transcriptional profiles of samples revealed that intratumoral $CD4^+$ and $CD8^+$ T_{conv} cells from T_{reg} cell-depleted animals clustered more strongly with T_{reg} cells than T_{conv} cells from T_{reg} cell-sufficient animals (Fig. 1E). Moreover, differences in gene expression between $CD4^+$ T_{conv} cells in the absence versus presence of T_{reg} cells were significantly positively correlated with differences in gene expression between intratumoral T_{reg} cells and $CD4^+$ T_{conv} cells from T_{reg} cell-sufficient animals (Fig. 1F). Collectively, these results show that intratumoral T_{conv} cells adopt a T_{reg} cell-like transcriptional profile upon experimental ablation of T_{reg} cells *in vivo*.

Ablation of T_{reg} cells promotes the induction of T_{conv} cell suppression

T_{reg} cells suppress the proliferation of naïve T_{conv} cells when co-cultured *in vitro* (37–39). Given their acquisition of a T_{reg} cell-like transcriptional profile, we asked whether T_{conv} cells develop suppressive function upon depletion of T_{reg} cells. To test this, we purified *Foxp3*$^{EGFP-}$ $CD4^+$ T_{conv} cells or *Foxp3*$^{EGFP+}$ $CD4^+$ T_{reg} cells by FACS from B16-F10-tumor bearing *Foxp3*$^{EGFP-DTR}$ mice and incubated them with congenically distinct naïve $CD4^+$ T_{conv} cells *in vitro* (Fig. 2A, Fig. S2). Strikingly, $CD4^+$ T_{conv} cells from the tumors of mice whose T_{reg} cells had been ablated by administration of DTx profoundly suppressed the proliferation of naïve $CD4^+$ T cell responders compared with $CD4^+$ T_{conv} cells from tumors of animals with intact T_{reg} cell populations (Fig. 2B and C). The level of suppression was only marginally less than the level of suppressive activity of a similar number of intratumoral $Foxp3^+$ T_{reg} cells. We observed lower levels of suppressive activity among splenic T_{conv} cells (Fig. S3A-B), suggesting that suppressive function was enriched in the tumor. In addition to suppressing T cell proliferation, T_{conv} cells from tumors of T_{reg} cell-depleted animals suppressed stimulation-driven induction of the activation marker CD44 on responder cells in contrast to T_{conv} cells from tumors of non-T_{reg} cell-depleted animals (Fig. 2D and E). T_{conv} cells from T_{reg} cell-depleted animals expressed similar levels of the co-inhibitory molecules TIGIT, TIM-3 and GITR to intratumoral T_{reg} cells (Fig. 2F and G). They also expressed higher levels of CTLA-4 and ICOS compared to $CD4^+$ T_{conv} cells from tumors with intact T_{reg} cell populations. Acquisition of suppressive function by T_{conv} cells was not an artefact of DTx treatment, since administration of DTx to *Foxp3*$^{EGFP-DTR}$ and control *Foxp3*^{EGFP} mice resulted in induction of potent suppressive activity only among $CD4^+$ T_{conv} cells from *Foxp3*$^{EGFP-DTR}$ animals, whose T_{reg} cells are sensitive to DTx treatment (Fig. S3C-D). Thus, upon T_{reg} cell ablation, $CD4^+$ T_{conv} cells within tumors acquire transcriptional and functional characteristics of T_{reg} cells.

Europe PMC Funders Author Manuscripts

Europe PMC Funders Author Manuscripts

T_{reg} cell depletion results in activation and expansion of CCR8$^+$ T_{conv} cells

To understand whether changes in the transcriptional and functional properties of bulk populations of T_{conv} cells in the absence of T_{reg} cells were driven by specific subpopulations, we performed scRNA-Seq of bulk T cell populations sorted by FACS from B16-F10 melanoma tumors of DTx- and PBS-treated *Foxp3*$^{EGFP\text{-}DTR}$ animals at day 16 after tumor implantation. Single-cell gene expression data were clustered using Seurat and global transcriptional differences between cells were visualized in two-dimensional space using Uniform Manifold Approximation and Projection (UMAP). *k*-means clustering revealed the presence of 8 transcriptionally distinct clusters of cells (Fig. 3A). Clusters 2 and 3 were enriched in control samples, whereas Clusters 0, 1, 5 and 7 were enriched among T cells from tumors of T_{reg} cell-depleted animals (Fig. 3B and C). Enrichment analysis was used to determine which cell cluster was most responsible for the induction of T_{reg} cell-like gene expression within bulk RNA-Seq profiles of T_{conv} cells from T_{reg} cell-depleted animals. This revealed that Cluster 0 (present at a ~3:1 ratio in the DTx treatment condition) was most enriched in genes specifically upregulated by CD4$^+$ T_{conv} cells upon DTx treatment (Fig. 3D). To define surface markers which would enable isolation of cells of Cluster 0, we performed an analysis of uniquely upregulated transcripts within each cluster. This analysis revealed that Cluster 0 cells express transcripts associated with T cell activation but which are also highly expressed by T_{reg} cells, including *Il2ra, Tigit* and *Tnfrsf4* (Fig. 3E and Data file S3). Strikingly, *Ccr8* mRNA expression was also upregulated in Cluster 0 cells upon depletion of T_{reg} cells, which was notable since we and others have shown that chemokine (C-C motif) receptor 8 (CCR8) marks highly suppressive T_{reg} cells under steady-state conditions within both murine and human tumors (40–44). A focused analysis of the CD4$^+$ T cells in Cluster 0 revealed a sub-population of cells (subcluster 5) enriched in expression of transcripts encoding proteins associated with Th2 differentiation, including *Ccr8, Gata3, Maf* and *Il10*, and suppressive/co-inhibitory function, including *Pdcd1, Tigit, Il10* and *Lag3* (Fig. S4, Data file S4). Accordingly, an analysis of the distribution of cells expressing *Ccr8, Il2ra, Tigit* and *Tnfrsf4* revealed that while in T_{reg} cell-replete animals, these markers are largely expressed by intratumoral of *Foxp3*$^{EGFP+}$ T_{reg} cells, they became expressed by a subset of *Foxp3*$^{EGFP-}$ CD4$^+$ T_{conv} cells upon T_{reg} cell depletion (Fig. 3F and Fig. S5).

We therefore analyzed the expression of CCR8 on the surface of T_{reg} and T_{conv} cells in tumors and lymphatics of *Foxp3*$^{EGFP\text{-}DTR}$ animals treated with PBS or DTx (Fig. 3G and H). We found that T_{reg} cell depletion increased the absolute number of CCR8$^+$ T_{conv} cells within all tissues analyzed, including tumors, draining lymph nodes (dLN) and spleen, whereas the relative frequency of CCR8$^+$ cells among total CD4$^+$ *Foxp3*$^{EGFP-}$ T_{conv} cells was increased within the spleens of T_{reg} cell-depleted animals, but not within dLN and tumors due to the absolute expansion of other CD4$^+$ *Foxp3*$^{EGFP-}$ T_{conv} cells subsets in these tissues upon T_{reg} cell depletion.

CCR8 expression marks highly suppressive T_{conv} cells within tumors

To better understand the identity of CCR8$^+$ T_{conv} cells, we purified CCR8$^+$ and CCR8$^-$ CD4$^+$ T_{conv} cells by FACS from B16-F10 tumors of DTX-treated *Foxp3*$^{EGFP\text{-}DTR}$ mice and subjected them to bulk RNA-Seq. CCR8$^+$ T_{conv} cells were enriched in transcripts encoding

Europe PMC Funders Author Manuscripts

Europe PMC Funders Author Manuscripts

molecules associated with both T cell activation such as *Tnfrsf9* (encoding 4-1BB) and T_{reg} cell suppressive function, including *Il2ra, Areg*, and *Il10* (Fig. 4A and Data file S5). Interestingly, $CCR8^+$ T_{conv} cells were not enriched in transcripts associated with suppressive type 1 regulatory T cells (Tr1) such as *Eomes, Gzmk, Itga2* (encoding CD49b), *Ccr5*, or *Cd226*, suggesting that they are distinct from Tr1 cells. Gene set enrichment analysis (GSEA) of global gene expression differences between $CCR8^+$ and $CCR8^-$ T_{conv} cells revealed a negative enrichment of genes upregulated in *Foxp3*$^-$ T_{conv} cells *vs Foxp3*$^+$ T_{reg} cells among $CCR8^+$ T_{conv} cells compared with $CCR8^-$ T_{conv} cells (Fig. 4B). Consistently, we observed that global differences in gene expression between $CCR8^+$ and $CCR8^-$ T_{conv} cells were positively correlated with global differences in gene expression between intratumoral T_{reg} and T_{conv} cells (Fig. 4C), further suggesting that $CCR8^+$ *Foxp3*$^-$ T_{conv} cells possess a T_{reg} cell-like transcriptional profile.

We compared the phenotype of $CCR8^-$ and $CCR8^+$ $CD4^+$ T_{conv} cells from tumors of mice whose T_{reg} cells had been depleted by DTx with that of T_{reg} cells. Like T_{reg} cells, we found that $CCR8^+$ $CD4^+$ T_{conv} cells expressed high levels of CD25, OX40, GITR, TIGIT and LAG-3 compared to $CCR8^-$ $CD4^+$ T_{conv} cells (Fig. 4D and E). $CCR8^+$ T_{conv} cells also expressed increased levels of the transcription factor GATA3, suggesting that they possess a Th2-like differentiation state. To test whether the accumulation of $CCR8^+$ cells within intratumoral T_{conv} cell populations following T_{reg} cell ablation accounts for their increased suppressive activity, we separately sorted $CCR8^+$ and $CCR8^-$ *Foxp3*$^{EGFP-}$ T_{conv} cells from the tumors of DTx-treated *Foxp3*$^{EGFP\text{-}DTR}$ mice and assessed their ability to suppress naïve T_{conv} cell proliferation *in vitro*. Notably, suppressive function was enriched within the $CCR8^+$ T_{conv} cell fraction, which were more capable of restricting proliferation of responder cells compared to the $CCR8^-$ T_{conv} cell fraction (Fig. 4F and G). Taken together, these results suggest that CCR8 expression marks a subset of highly activated and suppressive T_{conv} cells which accumulate systemically and within tumors upon T_{reg} cell depletion.

$CD4^+$ $FOXP3^-$ $CCR8^+$ T_{conv} cells are found within tumors of NSCLC patients

In order to determine if $CCR8^+$ $FOXP3^-$ T_{conv} cells are enriched in human tumors, we analyzed $CD4^+$ T cells from 48 patents with non-small cell lung carcinoma (NSCLC) by flow cytometry (Fig. S6). Similar to our observations in mouse, $CCR8^+$ $FOXP3^-$ T_{conv} cells expressed high levels of CD25 and were significantly enriched in tumor tissue compared to healthy adjacent tissue and blood from the same patients (Fig. 5A and 5B). Moreover, the frequency of $CCR8^+$ $CD25^+$ $FOXP3^-$ T_{conv} cells was inversely correlated with the frequency of cytotoxic $CD8^+$ T cells within tumors (Fig. 5C). They also co-expressed the inhibitory receptors PD-1, TIGIT and TIM-3 (Fig. 5D and E). $CD4^+$ $FOXP3^-$ $CCR8^+$ T cells displayed increased expression of the tissue-residency marker CXCR6 and co-stimulatory receptor CD27 compared to $CCR8^-$ cells and their phenotype was largely overlapping with that of $FOXP3^+$ T_{reg} cells (Fig. 5E and F). $CD4^+$ $FOXP3^-$ $CCR8^+$ T cells lacked expression of EOMES and Granzyme K, providing further evidence that this cell type is distinct from Tr1 cells (Fig. 5E). The presence of $CCR8^+$ $FOXP3^-$ T_{conv} cells in human tumors under steady-state conditions and without T_{reg} cell depletion is consistent with our observations within murine tumors (Fig. 3H and I), which contain a population of $CCR8^+$ $CD4^+$ T_{conv} cells under basal conditions that undergo substantial expansion upon T_{reg} cell ablation.

Europe PMC Funders Author Manuscripts

Europe PMC Funders Author Manuscripts

IL-10-dependent immune suppression by T_{conv} cells limits efficacy of T_{reg} cell depletion

We sought to understand how intratumoral $CD4^+$ T_{conv} cells exert their suppressive function. Informed by the results of our transcriptional analyses, we screened for the involvement of candidate suppressive mechanisms by which T_{conv} cells from T_{reg} cell-depleted animals suppress T cell activation and proliferation *in vitro*. We tested whether blocking antibodies directed against CD25, CTLA-4, IL-10 receptor (IL-10R) and CCR8, neutralizing antibodies specific for transforming growth factor (TGF)-β, or pharmacological inhibition of steroid biosynthesis preferentially produced by Th2 cells using aminoglutethimide (AG) (45), are able to reverse the suppressive activity of intratumoral T_{conv} cells from T_{reg} cell-depleted animals. Importantly, while the proliferation of naïve $CD4^+$ T cells was suppressed by $Foxp3^-$ T_{conv} cells, these differences induced by the presence of suppressive $Foxp3^-$ T_{conv} cells were abolished upon treatment of cells with anti-IL-10R (Fig. 6A and B).

Given these observations, we asked whether $CCR8^+$ T_{conv} cells are primary producers of *Il10* mRNA upon depletion of T_{reg} cells. We first examined whether the expression of *Il10* mRNA is co-correlated with the expression of *Ccr8* mRNA, and therefore co-expressed within the same cells, using scRNA-Seq of T cells from tumors of T_{reg} cell-replete and -depleted animals. Since IL-10 is known to be produced by $CD4^+$ T_R1 cells which express LAG3 and CD49b (46–49), $Eomes^+$ $CD4^+$ T_{conv} cells (50–52), exhausted $CD8^+$ T cells which express PD-1 (53) and $CD4^+$ Th2 cells which express GATA3, IL-4 and IL-13 (54, 55), we included the genes encoding these and other markers in our co-correlation analysis. We found that under steady-state (T_{reg} cell-replete) conditions, *Il10* formed a predominant co-correlation cluster with *Cd8a, Pdcd1, Ifng, Tnf*, and *Eomes* but also a smaller cluster containing *Gata3* and *Foxp3*, suggesting that $CD8^+$ T cells in differential states of exhaustion, and Th2-like T_{reg} cells are a predominant source of IL-10 (Fig. 6C). However, we found that T_{reg} cell depletion resulted in a striking change in the co-correlation relationship of *Il10* mRNA with the other genes examined, forming a predominant cluster of co-correlated genes containing *Cd4, Ccr8, Il13, Il14* and *Gata3*. These results suggested that upon T_{reg} cell ablation, the source of *Il10* shifts to the previously identified $CD4^+$ $CCR8^+$ T_{conv} cell subset with Th2-like characteristics, and that $CD4^+$ $CCR8^+$ T_{conv} cells undergo activation into *Il10*-expressing cells. To confirm this, we sorted $CCR8^-$ and $CCR8^+$ T_{conv} cells from tumors of T_{reg} cell-replete and -depleted animals and subjected them to qRT-PCR. We found that *Il10* mRNA expression was enriched among $CCR8^+$ T_{conv} cells from T_{reg} cell-depleted animals compared with both $CCR8^-$ cells from T_{reg} cell-depleted animals and $CCR8^+$ or $CCR8^-$ cells from T_{reg} cell-replete animals (Fig. 6D). These findings supported the hypothesis that $CCR8^+$ T_{conv} cells become the predominant source of T cell-expressed IL-10 upon T_{reg} cell depletion.

We therefore asked whether T_{reg} cell depletion triggers induction of IL-10-dependent suppressive activity among $Foxp3^-$ T_{conv} cells, limiting efficacy of T_{reg} cell depletion *in vivo*. We had observed that T_{reg} cell depletion was ineffective at significantly reducing growth of established B16 tumors, while T_{reg} cell depletion during early disease delayed tumor growth but was ineffective at inducing complete responses (Fig. 1A). To test whether IL-10 production by T_{conv} cells is responsible for resistance to T_{reg} cell-depleting therapy *in vivo*, we generated $Il10^{flox/flox}$ $Cd4^{Cre}$ $Foxp3^{EGFP\text{-}DTR}$ and littermate $Cd4^{Cre}$

Europe PMC Funders Author Manuscripts

Europe PMC Funders Author Manuscripts

Foxp3$^{EGFP\text{-}DTR}$ (IL-10 proficient) control mice. This allowed us to examine the effect of T_{reg} cell depletion in animals whose remaining T cells can or cannot produce IL-10. Since IL-10 ablation has been shown to promote tumor growth under steady-state conditions (56, 57), we subcutaneously implanted with B16-F10 cells into *Il10*$^{flox/flox}$ *Cd4*^{Cre} *Foxp3*$^{EGFP\text{-}DTR}$ and littermate *Cd4*^{Cre} *Foxp3*$^{EGFP\text{-}DTR}$ control animals and selected animals with tumors of similar size (range 12 - 64 mm^2) at day 10 after tumor implantation for randomization to treatment groups (PBS or DTx). We found that conditional deletion of IL-10 within T cells resulted in loss of resistance to T_{reg} cell depletion, as indicated by reduced tumor growth when T_{reg} cells were ablated in animals lacking T cell-restricted IL-10 expression, but not when either condition was present alone (Fig. 6E). There was also an increase in expression of the activation marker CD44 on $CD4^+$ T_{conv} cells and $CD8^+$ T cells from animals bearing a conditional deletion of *Il10* and whose T_{reg} cells had been ablated (Fig. 6F). T_{reg} cell ablation in animals bearing a conditional deletion of *Il10* within T cells was associated with increased frequencies of $CD8^+$ T cells and $CD4^+$ T_{conv} cells expressing the cytokines IFN-γ and TNF (Fig. 6G and H). These results demonstrate a critical role for T cell-produced IL-10 in resistance to T_{reg} cell depletion.

Blockade of IL-10 signaling synergizes with T_{reg} cell depletion to induce robust anti-tumor immune responses

We next asked whether antibody blockade of IL-10 signaling synergizes with T_{reg} cell depletion *in vivo*. We tested whether blockade of IL-10R using anti-IL-10R antibodies reverses resistance to T_{reg} cell-depleting therapy. We found that late T_{reg} cell depletion or IL-10R blockade alone failed to drive significant reduction in tumor growth, whereas their combination resulted in potent tumor regression (Fig. 7A). Moreover, IL-10 blockade synergized with early T_{reg} cell ablation to induce complete responses in a proportion of animals receiving combined therapy (Fig. S7). We found that IL-10R blockade both alone and in combination with T_{reg} cell depletion increased the ratio of $CD8^+$ T cells expressing IFN-γ and TNF within tumors, but the absolute number of IFN-γ- and TNF-expressing $CD8^+$ T cells was markedly increased upon combined T_{reg} cell ablation and IL-10R blockade, reflecting a combination of increased T cell infiltration and cytokine production (Fig. 7B and C). Similarly, the combination of T_{reg} cell depletion and IL-10R blockade resulted in an increase in the frequency and absolute number of IFN-γ- and TNF-expressing $CD4^+$ T cells (Fig. 7D and E). These findings demonstrate that T_{conv} cells within tumors adopt IL-10 dependent suppressive activity upon therapeutic elimination of T_{reg} cells. This contributes to treatment failure of T_{reg} cell depleting immunotherapies and that combined targeting of T_{reg} cells and compensatory IL-10-dependent suppression invoked upon their depletion may enhance therapy.

Discussion

T_{conv} cells and T_{reg} cells share components of their activation programs to meet similar metabolic, proliferative and migratory requirements as they transition from quiescent states to activated states (58–60). A substantial effort is now underway to develop therapies that specifically target molecules that distinguish T_{reg} cells within tumors from their T_{conv} cell counterparts. These efforts have been informed by comparative analyses of the molecular

Europe PMC Funders Author Manuscripts

Europe PMC Funders Author Manuscripts

profiles of T_{reg} cells and T_{conv} cells within tumors under steady-state conditions (61, 62). We compared the transcriptional profiles of T_{reg} cells with T_{conv} cells not only under steady-state conditions, but upon immune activation provoked by experimental T_{reg} cell ablation. This analysis revealed that T_{conv} cells adopt a highly similar transcriptional profile to T_{reg} cells upon T_{reg} cell depletion. The extent of this reprograming goes beyond what would be expected as a result of the shared properties of T_{reg} cell and T_{conv} cell core lymphocyte activation programs and reveals that T_{conv} cells take on compensatory IL-10-dependent suppressive function when T_{reg} cells are eliminated. Acquisition of a T_{reg} cell-like transcriptional profile by T_{conv} cells upon T_{reg} cell ablation suggests that in practice there are very few molecules whose targeting will enable highly specific depletion of T_{reg} cells within tumors. Nevertheless, a small cluster of genes was identified in our analyses which has an expression profile limited to T_{reg} cells compared with T_{conv} cells under both steady-state conditions and upon T_{reg} cell depletion. While this cluster of genes may contain targets for specific depletion of T_{reg} cells within tumors, a question raised by this study is whether specific depletion of T_{reg} cells is indeed desirable, rather than the targeting of molecules shared by T_{reg} cells and cells with compensatory suppressive function induced upon T_{reg} cell depletion.

It is known that CCR8 marks highly suppressive T_{reg} cells found in both mouse and human tumors (40–44, 63). There is significant interest in the development of therapies which deplete $CCR8^+$ T_{reg} cells within tumors. Given our observation that CCR8 also marks T_{conv} cells whose suppressive function is induced upon experimental T_{reg} cell ablation *in vivo*, it is reasonable to postulate that depletion of CCR8-expressing cells is a superior approach to T_{reg} cell depletion using other T_{reg} cell-expressed markers for induction of anti-tumor immunity, since CCR8-depleting therapies would target both T_{reg} cells and suppressive T_{conv} cells for destruction. It will be important to consider effects of CCR8-depleting therapies on both T_{reg} cells and $CCR8^+$ T_{conv} cells within tumors, both in pre-clinical investigations (42, 63), and if robust intratumoral depletion of $CCR8^+$ cells in the human clinical context is achieved. Alternatively, our data suggests that combining T_{reg} cell-targeted immunotherapies with blockade of IL-10 signaling will overcome compensatory suppression by T_{conv} cells.

It is interesting that the $CCR8^+$ T_{conv} cell subset observed in human tumors did not phenotypically overlap with previously described Tr1 cells within tumors. Suppressive Tr1 cells have been characterized in several human tumors including head neck and squamous cell carcinoma (HNSCC) (64), colorectal cancer (52, 65), hepatocellular carcinoma (49), Hodgkin lymphoma (66), metastatic melanoma (67) and non-small-cell lung cancer (52), and their presence is often associated with tumor progression. The suppressive subset of $CCR8^+$ T_{conv} cells we observe does not express EOMES or granzyme K, markers previously reported to be indicative of Tr1 cells. Recent studies have described a contribution of tumor-infiltrating follicular helper T (TFH) cells and follicular regulatory T (T_{FR}) cells to anti-tumor immunity (68, 69). However, CXCR5 was not expressed by $CCR8^+$ T_{conv} cells suggesting their distinction from T_{FH} cells. We did however observe high levels of GATA3 and *Il10* expression among $CCR8^+$ T_{conv} cells, suggesting that they represent a Th2-like subset expressing high levels of markers associated with T cell activation, including CD25, expanded systemically and within tumors upon T_{reg} cell depletion. Prior

Europe PMC Funders Author Manuscripts

Europe PMC Funders Author Manuscripts

work are consistent with these data, showing systemic expansion of Th2 cells expressing either GATA3 or Th2 cytokines upon experimental T_{reg} cell ablation (70, 71), and the intratumoral presence of $CD4^+$ T_{conv} cells expressing CCR8 (40–44, 63). We found that the frequency of $CCR8^+$ $CD25^+$ $FOXP3^-$ T_{conv} cells inversely correlates with the frequency of tumor-infiltrating $CD8^+$ T cells, suggesting that they play an inhibitory role in human tumor immunity. The observation that $CCR8^+$ T_{conv} cells expand and undergo activation to express IL-10 following depletion of T_{reg} cells provides an explanation of how bulk T_{conv} cells from tumors of T_{reg} cell-depleted animals acquire IL-10-dependent suppressive function despite lack of a change in the relative frequency of $CCR8^+$ cells within the tumor $CD4^+$ T_{conv} compartment. While our pre-clinical data from mouse models suggests that $CCR8^+$ T_{conv} cells expand numerically within tumors upon experimental T_{reg} cell ablation, this is difficult to formally assess in humans due to the lack of specific markers that are differentially expressed in comparison with $FOXP3^+$ T_{reg} cells, enabling their isolation *ex vivo*, and of clinically approved T_{reg} cell-depleting therapies in widespread use. However, a number of T_{reg} cell-targeted therapies are under development and it will be an important topic of future investigation to determine their effect upon $CCR8^+$ T_{conv} cells in humans. It will also be important to better define how $CCR8^+$ T_{conv} cells contribute to immune regulation in other contexts including infection and inflammation, as clones of $Foxp3^-$ $CD4^+$ T cells expressing CCR8, CD25 and IL-10 have previously been described in mice with experimental pulmonary granulomata (72), while $CD4^+$ T_{conv} cells expressing CCR8 are observed upon experimental allergic lung inflammation in mice (73), and infiltrating human skin (74).

Our findings show that in the context of T_{reg} cell depleting immunotherapies, IL-10 production by T_{conv} cells represents a secondary layer of immune suppression responsible for driving immunotherapy resistance. It is important that this immunosuppressive function of IL-10 in limiting the efficacy of T_{reg} cell targeted therapies is appreciated, since in other contexts, IL-10 has been shown to possess immunostimulatory activity both in pre-clinical models and in clinical trials (75–77). Our findings suggest that IL-10 blocking antibodies may be used as a synergistic therapy with T_{reg} cell-targeted immunotherapies to improve patient outcomes.

Preclinical studies suggest that T_{reg} cell depletion can reinvigorate T_{conv} cell responses, however clinical trials of T_{reg} cell depleting therapies have thus far been met with limited clinical efficacy (35, 78). While our analysis of human tumor-infiltrating $Foxp3^-$ T_{conv} cells revealed a fraction of $CCR8^+$ T_{conv} cells under steady-state conditions, it will be valuable to examine whether such cells are expanded upon immunotherapy with either novel T_{reg} cell-depleting therapies, or anti-CTLA-4 therapy, the therapeutic efficacy of which is postulated to in part depend upon depletion or blockade of the suppressive function of T_{reg} cells (79, 80), and indeed in the context of non-T_{reg} cell-targeted immunotherapy approaches. The prognostic significance of such cells in determining the outcome of the immunotherapy responses will reveal insights into their broader contribution to immunotherapy resistance.

Europe PMC Funders Author Manuscripts

Europe PMC Funders Author Manuscripts

Materials and Methods

Study design

The objective of this study was to understand how T_{reg} cell depletion affects the function and immunoregulatory capacity of the T cell lineage in the context of tumor immunity. We used the well-established *Foxp3*$^{EGFP\text{-}DTR}$ mouse to experimentally deplete T_{reg} cells in mice with syngeneic B16-F10 melanoma heterotopic tumors. We examined the consequences of T_{reg} cell depletion for tumor progression, as measured by blinded serial caliper measurements and tumor immunity, as assessed by scRNA-Seq and flow cytometry. We found that T_{conv} cells acquire T_{reg} cell-like suppressive functions upon depletion of T_{reg} cells. Using transcriptional profiling and *in vitro* suppression assays to better understand the nature of this suppressive activity, we found that this suppressive function was enriched among a Th2-like T_{conv} cell subset marked by expression of CCR8. Moreover, using antibody blockade and conditional *Il10* deletion experiments, we found that the suppressive activity induced upon T_{reg} cell depletion was dependent upon IL-10. The sample size for each experiment is specified in the figure legends. The number of independent experiments performed is stated in the figure legends. Age-matched male and female mice were randomly assigned to each group.

Mice

Foxp3$^{EGFP\text{-}DTR}$ mice were originally described by Kim et al. (36), *Foxp3*$^{IRES\text{-}EGFP}$, *Ptprc*^{a} (CD45.1), and *Rag2*$^{-/-}$ mice were obtained from the Jackson Laboratory. *Il10*$^{flox/flox}$ *and Cd4*^{Cre} mice (81) were obtained from Jean Langhorne (Francis Crick Institute) and crossed with *Foxp3*$^{EGFP\text{-}DTR}$ mice to generate *Il10*$^{flox/flox}$ *Cd4*^{Cre} *Foxp3*$^{EGFP\text{-}DTR}$ animals. Experiments were performed using 8-14 week old mice, with male and female mice equally distributed between experimental and control groups. Mice were housed at the University of Cambridge University Biomedical Services (UBS) Gurdon Institute Facility and Babraham Institute Biological Services Unit (BSU). Experiments were conducted in accordance with UK Home Office guidelines and were approved by University of Cambridge Animal Welfare and Ethics Review Board or by the Babraham Research Campus Animal Welfare and Ethics Review Board.

Human primary tissues

Primary tumors and adjacent healthy tissue were acquired from 48 NSCLC patients. Patients gave consent to be included in the study which was approved by the institutional review board of Humanitas Research Hospital (protocols no. 2578). Patients did not receive chemotherapy, radiotherapy or palliative surgery before samples were obtained. Samples were processed using the gentleMACS Dissociator (Miltenyi Biotec) into single cell suspensions as previously described (82), resuspended in dimethylsulfoxide (DMSO) with 10% Fetal Bovine Serum (FBS) and stored in liquid nitrogen.

Europe PMC Funders Author Manuscripts

Europe PMC Funders Author Manuscripts

High-dimensional flow cytometry analysis of human samples and computational processing of flow cytometric data

Samples were prepared for flow cytometry as previously described (82). Panels were developed according to an established protocol (83). Briefly, Flow Cytometry Standard (FCS) 3.0 files were analysed by standard gating in FlowJo version 9 to remove dead cells and cell aggregates, and identify $CD4^+$ $FOXP3^-$ T cells. 5,000 $CD4^+$ $FOXP3^-$ T cells per tumor sample (n = 48) were subsequently imported into FlowJo (version 10), biexponentially transformed, and exported in order to be analyzed by a custom-made publicly available pipeline of PhenoGraph (https://github.com/luglilab/Cytophenograph). A representative gating strategy is shown in Fig. S6. All samples were converted into comma separated value (CSV) files and concatenated in a single matrix by using the merge function of pandas package. The K value, indicating the number of nearest neighbors identified in the first iteration of the algorithm, was set at 500. Uniform Manifold Approximation and Projection (UMAP) was obtained by UMAP Python package.

Tumor challenge and treatment

Mice were injected subcutaneously in the left flank with 1.25×10^5 B16-F10 melanoma cells (ATCC). Tumors were measured at serial time points following implantation using digital calipers and tumor area was calculated as the length × width. Tumor measurements were completed by an independent investigator who was not aware of treatment groups or genotypes. For late DTx treatment experiments (starting day 10 post-tumor implantation), mice with tumors between 12 and 64 mm^2 at day 10 were randomized to treatment groups to reduce experimental variability. Mice were injected intraperitoneally (i.p) starting at the indicated time point with 1 μg of diphtheria toxin (DTx) every other day for a total of four injections and/or 250 μg of anti-IL-10R (clone 1B1.3A; BioXcell) daily for a total of 10 days. DTx from *Corynebacterium diphtheriae* (Sigma-Aldrich) was obtained in lyophilized powder form and reconstituted in sterile double-distilled water according to the manufacturer's instructions.

Suppression assays

The suppressive capacity of tumor T_{conv} cells and T_{reg} cells was measured *in vitro* as previously described (84). Briefly, $CD45.2^+$ $TCR\beta^+$ $CD4^+$ GFP^+ T_{reg} cells or $CD45.2^+$ $TCR\beta^+$ $CD4^+$ GFP^- T_{conv} cells were isolated from B16-F10 tumors of $Foxp3^{EGFP\text{-}DTR}$ mice treated with PBS or DTx using florescence-activated cell sorting (FACS) 16 days post implantation and used as suppressor cells. A representative gating strategy is shown in shown in Fig. S2. Naïve $CD4^+$ T_{conv} cells ($CD25^-$ $CD44^-$ $CD62L^+$) were purified from the spleens of WT CD45.1 mice by FACS and stained with CellTrace Violet™ (CTV) according to the manufacturer's protocol (Thermo Fisher Scientific) and used as responder T (T_{resp}) cells. 2.5×10^4 or 1.25×10^4 (as indicated) suppressor $CD4^+$ T_{reg} cells or T_{conv} cells were co-cultured with 1×10^5 naïve responder T cells in the presence of anti-CD3 (BioLegend 1 μg/mL) and 5.0×10^4 $Rag2^{-/-}$ antigen presenting cells (APCs). T_{resp} cells cultured in the presence of anti-CD3 and APCs but without tumor T_{reg} cells or T_{conv} cells were used as a control. Cell division was evaluated by flow cytometry after 4 days of culture. For the screen, cells were cultured alone (gray) or with suppressors (purple) and

Europe PMC Funders Author Manuscripts

Europe PMC Funders Author Manuscripts

with Aminoglutethimide (AG) at a final concentration of 125μM or with other indicated reagents at a final concentration of 10μg/mL.

Flow cytometry of murine samples

Tumor samples were digested using collagenase and DNase for 30 minutes at 37 °C. Percoll was used to isolate lymphocytes from tumors. Tumors and spleens were mechanically dissociated over a 40 μm cell strainer. Red blood cells were lysed using ACK Lysing Buffer (Gibco). Cells were stained with the Fixable Viability Dye eFluor™ 780 (Thermo Fisher Scientific), Viakrome 808 (Beckman Coulter), or DAPI (Sigma) to discriminate between live and dead cells and then incubated with FC block (BioXcell, 2.4G2) the following surface antibodies for 30 minutes on ice: anti-TCRβ FITC (H57-597), anti-CD8 BV605 (53-6.7), anti-TIM-3 BV421 (RMT3-23), anti-CCR8 BV421 (SA214G2), anti-OX40 BV711 (OX-86), anti-TIGIT PE (4D4/mTIGIT), anti-ICOS BV750 (C398.4A), anti-LAG-3 BV785 (C9B7W), anti-CD3ε Spark Blue 550 (17A2) from Biolegend, anti-CD25 PE-Cyanine7 (PC61.5), anti-CD44 PerCP-Cyanine5.5 (IM7), anti-CD45.1 APC (A20), anti-CD4 PE-Cy7 (RM4-5) from eBioscience, and anti-GITR BUV805 (DTA-1), anti-CD4 BUV395 or BUV496 (GK1.5) from BD Biosciences. Cells were stimulated with phorbol 12-myristate 13-acetate (PMA) and ionomycin and blocked with brefeldin A (BFA) for 4 hours in RPMI 1640 complete medium. The intracellular antibodies anti-Foxp3 APC (FJK-16S), anti-IFN-γ PerCPCy5.5 (XMG1.2), anti-GATA3 PE-eFluor610 (TWAJ) were purchased from eBioscience, and anti-CTLA-4 BV605 (UC10-4B9), anti-TNF PE-Cy7 (MP6-XT22) were purchased from BioLegend and used with the eBioscience Foxp3/Transcription Factor Staining Buffer Set (Invitrogen, Thermo Fisher Scientific) according to the manufacturer's protocol. For determination of CCR8 expression by Foxp3^{-} T_{conv} cells, cells from tumor-bearing *Foxp3*$^{EGFP\text{-}DTR}$ animals were surface-stained and analyzed unfixed using flow cytometry, with EGFP expression used to discriminate T_{reg} cells and T_{conv} cells. Samples were analyzed using BD Fortessa, Beckman Coulter CytoFLEX, and Cytek® Aurora analyzers. After analysis, data were analyzed using FlowJo software (Tree Star, Inc.).

scRNA Sequencing and analysis

Single cell suspensions of T cells were purified by total pan T cell enrichment (Invitrogen/Thermo Fisher Scientific), and live TCRβ^{+} cells were sorted from B16 tumors by FACS 16 days post implantation. RNA libraries were prepared for single cell RNA sequencing (scRNA-Seq) using the Chromium Single Cell 5' Library & Gel Bead Kit v2 (10x Genomics) processed with Chromium (10x Genomics), and sequenced using the HiSeq 4000 System (Illumnia). Raw 10x sequencing data were processed as previously described and mapped to mm10. We confirmed that cells were sequenced to saturation. Data were merged with cell ranger aggr (cellranger-v5.0.0). Merged data were transferred to the R statistical environment for analysis primarily using the package Seurat (v3.2.2) in R v4.0.3. The analysis included only cells expressing between 200 and 2,500 genes, <5% mitochondrial-associated transcripts, and genes expressed in at least three cells. The data were then log-normalized and scaled per cell, and variable genes were detected using the FindVariableFeatures function in Seurat, as per default settings, using 2000 features and further processed as per the ScaleData function. Principal component analysis (PCA) was run on the variable genes, and the first six principal components (PCs) were selected

Europe PMC Funders Author Manuscripts

Europe PMC Funders Author Manuscripts

for further analyses, based on the standard deviation of the PCs, as determined by an "elbow plot" in Seurat. Cells were clustered using the FindClusters function in Seurat with default settings, resolution = 0.5, and six PCs. UMAP was calculated using six PCs (RunUMAP function). For broadly defining the transcriptional features of each cluster, the FindAllMarkers function (only.pos = FALSE, min.pct = 0.1, thresh.use = 0.2, test.use = "MAST") was used, and the associated heatmap was generated using the DoHeatmap function using up to the top 10 transcripts identified per cluster as defined by FindAllMarkers. The transcriptomic score of a particular cluster was calculated using the AddModuleScore function with default settings. Further visualizations of exported normalized data were generated using the Seurat RidgePlot functions and custom R scripts.

RNA Sequencing and analysis

Single-cell suspensions were purified by FACS (as described above) 16 days post tumor implantation, and stored in 40 μl RNA*later*™ Stabilization Solution at -80 °C. RNA was extracted from samples using the RNeasy Plus Mini Kit (Qiagen) with optional QIAshredder step according to the manufacturer's protocol. RNA-Sequencing (RNA-Seq) analyses were performed using ≥ 2 biological replicates. RNA-Seq was performed and analyzed as described previously (59). RNA Libraries were prepared using the Clontech SMARTer Ultra Low-input RNA kit (Takara) and sequenced on an Illumina HiSeq 2500 instrument using Illumina TruSeq v4.0 chemistry. The resulting FastQ files underwent quality control with FastQC, adaptor trimming with Cutadapt and alignment to the NCBIM37 *Mus musculus* genome annotation with hisat2 using ClusterFlow pipelines. Uniquely mapped reads were used to calculate gene expression and FPM values normalized to total library size with intergenic read normalization were calculated. Differential expression and statistical significance were calculated using the Wald test with adjustment for multiple testing using the Benjamini-Hochberg method using DESeq2 (85). Differentially expressed genes were further analyzed using R. PCA was performed using R *plotPCA* with count data transformed using variance stabilizing transformation (VST) from fitted dispersion-mean relationships generated using DESeq2 *vst*. Expression heatmaps were generated using FPM values normalized to row maxima using the R *pheatmap* package. Hierarchical clustering was performed using the Ward method. Dendrograms were cut at levels sufficient to allow 3-5 clusters to be discriminated.

Statistical Analysis

Statistical analysis was performed using Graphpad Prism software. Two-tailed Student's *t* tests or one-way ordinary ANOVAs were used as indicated to calculate statistical significance of the difference in sample means. *P* values of less than 0.05 were considered statistically significant. Statistical tests used are specified in the figure legends. In all figures, data represent the mean ± the standard error of the mean (SEM) or standard deviation (SD) as indicated. *P* values correlate with symbols as follows: ns = not significant, * $P \leq 0.05$, ** $P \leq 0.01$, *** $P \leq 0.001$, **** $P \leq 0.0001$.

Supplementary Material

Refer to Web version on PubMed Central for supplementary material.

Europe PMC Funders Author Manuscripts

Europe PMC Funders Author Manuscripts

Acknowledgements

We thank members of the University of Cambridge UBS Gurdon Facility and Babraham Institute Biological Services Facility for technical support with animal experiments. The authors gratefully acknowledge the flow cytometry facility from the School of the Biological Sciences for their support and assistance in this work, and Dr. Simone Puccio (Humanitas) for help with computational analyses, and the members of the high-throughput sequencing facilities. We thank staff at the CRUK Cambridge Institute sequencing facility for their assistance with single-cell RNA-Seq. We thank members of the Roychoudhuri laboratory for sharing of reagents, protocols, ideas and discussion. We apologize to those authors whose work we were unable to reference due to space restrictions.

Funding

The research was supported by the UK Medical Research Council (MRC; grant MR/S024468/1), the Wellcome Trust / Royal Society (grant 105663/Z/14/Z), Cancer Research UK (grant C52623/A22597), the Italian Ministry of Health (Grant Giovani Ricercatori GR-2018-12367258 to E.L.). E.L. is a CRI Llyod J. Old STAR (CRI award 3914).

Data and materials availability

All bulk RNA-Seq and scRNA-Seq data will be made publicly available under NCBI Gene Expression Omnibus (GEO) accession number GSE236825. All other data needed to support the conclusions of the paper are present in the paper or the Supplementary Materials.

References

1. Hodi FS, O'Day SJ, McDermott DF, Weber RW, Sosman JA, Haanen JB, Gonzalez R, Robert C, Schadendorf D, Hassel JC, Akerley W, et al. Improved survival with ipilimumab in patients with metastatic melanoma. N Engl J Med. 2010; 363: 711–723. [PubMed: 20525992]
2. Robert C, Thomas L, Bondarenko I, O'Day S, Weber J, Garbe C, Lebbe C, Baurain JF, Testori A, Grob JJ, Davidson N, et al. Ipilimumab plus dacarbazine for previously untreated metastatic melanoma. N Engl J Med. 2011; 364: 2517–2526. [PubMed: 21639810]
3. Gubin MM, Zhang X, Schuster H, Caron E, Ward JP, Noguchi T, Ivanova Y, Hundal J, Arthur CD, Krebber WJ, Mulder GE, et al. Checkpoint blockade cancer immunotherapy targets tumour-specific mutant antigens. Nature. 2014; 515: 577–581. [PubMed: 25428507]
4. Larkin J, Lao CD, Urba WJ, McDermott DF, Horak C, Jiang J, Wolchok JD. Efficacy and Safety of Nivolumab in Patients With BRAF V600 Mutant and BRAF Wild-Type Advanced Melanoma: A Pooled Analysis of 4 Clinical Trials. JAMA Oncol. 2015; 1: 433–440. [PubMed: 26181250]
5. Larkin J, Chiarion-Sileni V, Gonzalez R, Grob JJ, Cowey CL, Lao CD, Schadendorf D, Dummer R, Smylie M, Rutkowski P, Ferrucci PF, et al. Combined Nivolumab and Ipilimumab or Monotherapy in Untreated Melanoma. N Engl J Med. 2015; 373: 23–34. [PubMed: 26027431]
6. Sharma P, Hu-Lieskovan S, Wargo JA, Ribas A. Primary, Adaptive, and Acquired Resistance to Cancer Immunotherapy. Cell. 2017; 168: 707–723. [PubMed: 28187290]
7. Reck M, Rodriguez-Abreu D, Robinson AG, Hui R, Csoszi T, Fulop A, Gottfried M, Peled N, Tafreshi A, Cuffe S, O'Brien M, Rao S, et al. K.-. Investigators, Pembrolizumab versus Chemotherapy for PD-L1-Positive Non-Small-Cell Lung Cancer. N Engl JMed. 2016; 375: 1823–1833. [PubMed: 27718847]
8. Hamid O, Molinero L, Bolen CR, Sosman JA, Munoz-Couselo E, Kluger HM, McDermott DF, Powderly JD, Sarkar I, Ballinger M, Fasso M, et al. Safety, Clinical Activity, and Biological Correlates of Response in Patients with Metastatic Melanoma: Results from a Phase I Trial of Atezolizumab. Clin Cancer Res. 2019; 25: 6061–6072. [PubMed: 31358540]
9. Plitas G, Rudensky AY. Regulatory T Cells in Cancer. Annual Review of Cancer Biology. 2020; 4: 459–477.
10. De Peaux K, Delgoffe GM. Metabolic barriers to cancer immunotherapy. Nature review Immunologys. 2021.
11. Sakaguchi S, Mikami N, Wing JB, Tanaka A, Ichiyama K, Ohkura N. Regulatory T Cells and Human Disease. Annu Rev Immunol. 2020; 38: 541–566. [PubMed: 32017635]

Europe PMC Funders Author Manuscripts

12. Gallimore A, Quezada SA, Roychoudhuri R. Regulatory T cells in cancer: where are we now? Immunology. 2019; 157: 187–189. [PubMed: 31225653]
13. Stockis J, Roychoudhuri R, Halim TYF. Regulation of regulatory T cells in cancer. Immunology. 2019; 157: 219–231. [PubMed: 31032905]
14. Roychoudhuri R, Eil RL, Restifo NP. The interplay of effector and regulatory T cells in cancer. Curr Opin Immunol. 2015; 33: 101–111. [PubMed: 25728990]
15. Sato E, Olson SH, Ahn J, Bundy B, Nishikawa H, Qian F, Jungbluth AA, Frosina D, Gnjatic S, Ambrosone C, Kepner J, et al. Intraepithelial CD8+ tumor-infiltrating lymphocytes and a high CD8+/regulatory T cell ratio are associated with favorable prognosis in ovarian cancer. Proc Natl Acad Sci U S A. 2005; 102: 18538–18543. [PubMed: 16344461]
16. Curiel TJ, Coukos G, Zou L, Alvarez X, Cheng P, Mottram P, Evdemon-Hogan M, Conejo-Garcia JR, Zhang L, Burow M, Zhu Y, et al. Specific recruitment of regulatory T cells in ovarian carcinoma fosters immune privilege and predicts reduced survival. Nat Med. 2004; 10: 942–949. [PubMed: 15322536]
17. Bates GJ, Fox SB, Han C, Leek RD, Garcia JF, Harris AL, Banham AH. Quantification of regulatory T cells enables the identification of high-risk breast cancer patients and those at risk of late relapse. J Clin Oncol. 2006; 24: 5373–5380. [PubMed: 17135638]
18. Petersen RP, Campa MJ, Sperlazza J, Conlon D, Joshi MB, Harpole DH Jr, Patz EF Jr. Tumor infiltrating Foxp3+ regulatory T-cells are associated with recurrence in pathologic stage I NSCLC patients. Cancer. 2006; 107: 2866–2872. [PubMed: 17099880]
19. Gao Q, Qiu SJ, Fan J, Zhou J, Wang XY, Xiao YS, Xu Y, Li YW, Tang ZY. Intratumoral balance of regulatory and cytotoxic T cells is associated with prognosis of hepatocellular carcinoma after resection. J Clin Oncol. 2007; 25: 2586–2593. [PubMed: 17577038]
20. Griffiths RW, Elkord E, Gilham DE, Ramani V, Clarke N, Stern PL, Hawkins RE. Frequency of regulatory T cells in renal cell carcinoma patients and investigation of correlation with survival. Cancer Immunol Immunother. 2007; 56: 1743–1753. [PubMed: 17487490]
21. Hiraoka N, Onozato K, Kosuge T, Hirohashi S. Prevalence of FOXP3+ regulatory T cells increases during the progression of pancreatic ductal adenocarcinoma and its premalignant lesions. Clin Cancer Res. 2006; 12: 5423–5434. [PubMed: 17000676]
22. Perrone G, Ruffini PA, Catalano V, Spino C, Santini D, Muretto P, Spoto C, Zingaretti C, Sisti V, Alessandroni P, Giordani P, et al. Intratumoural FOXP3-positive regulatory T cells are associated with adverse prognosis in radically resected gastric cancer. Eur J Cancer. 2008; 44: 1875–1882. [PubMed: 18617393]
23. Jordanova ES, Gorter A, Ayachi O, Prins F, Durrant LG, Kenter GG, van der Burg SH, Fleuren GJ. Human leukocyte antigen class I, MHC class I chain-related molecule A, and CD8+/regulatory T-cell ratio: which variable determines survival of cervical cancer patients? Clin Cancer Res. 2008; 14: 2028–2035. [PubMed: 18381941]
24. Alvisi G, Termanini A, Soldani C, Portale F, Carriero R, Pilipow K, Costa G, Polidoro M, Franceschini B, Malenica I, Puccio S, et al. Multimodal single-cell profiling of intrahepatic cholangiocarcinoma defines hyperactivated Tregs as a potential therapeutic target. J Hepatol. 2022; 77: 1359–1372. [PubMed: 35738508]
25. Sinicrope FA, Rego RL, Ansell SM, Knutson KL, Foster NR, Sargent DJ. Intraepithelial effector (CD3+)/regulatory (FoxP3+) T-cell ratio predicts a clinical outcome of human colon carcinoma. Gastroenterology. 2009; 137: 1270–1279. [PubMed: 19577568]
26. Maj T, Wang W, Crespo J, Zhang H, Wang W, Wei S, Zhao L, Vatan L, Shao I, Szeliga W, Lyssiotis C, et al. Oxidative stress controls regulatory T cell apoptosis and suppressor activity and PD-L1-blockade resistance in tumor. Nat Immunol. 2017; 18: 1332–1341. [PubMed: 29083399]
27. Simpson TR, Li F, Montalvo-Ortiz W, Sepulveda MA, Bergerhoff K, Arce F, Roddie C, Henry JY, Yagita H, Wolchok JD, Peggs KS, et al. Fc-dependent depletion of tumor-infiltrating regulatory T cells co-defines the efficacy of anti-CTLA-4 therapy against melanoma. J Exp Med. 2013; 210: 1695–1710. [PubMed: 23897981]
28. Yu P, Lee Y, Liu W, Krausz T, Chong A, Schreiber H, Fu YX. Intratumor depletion of CD4+ cells unmasks tumor immunogenicity leading to the rejection of late-stage tumors. J Exp Med. 2005; 201: 779–791. [PubMed: 15753211]

Europe PMC Funders Author Manuscripts

Europe PMC Funders Author Manuscripts

29. Liu C, Workman CJ, Vignali DA. Targeting regulatory T cells in tumors. FEBS J. 2016; 283: 2731–2748. [PubMed: 26787424]
30. Jacobs JF, Punt CJ, Lesterhuis WJ, Sutmuller RP, Brouwer HM, Scharenborg NM, Klasen IS, Hilbrands LB, Figdor CG, de Vries IJ, Adema GJ. Dendritic cell vaccination in combination with anti-CD25 monoclonal antibody treatment: a phase I/II study in metastatic melanoma patients. Clin Cancer Res. 2010; 16: 5067–5078. [PubMed: 20736326]
31. Sampson JH, Schmittling RJ, Archer GE, Congdon KL, Nair SK, Reap EA, Desjardins A, Friedman AH, Friedman HS, Herndon JE 2nd, Coan A, et al. A pilot study of IL-2Ralpha blockade during lymphopenia depletes regulatory T-cells and correlates with enhanced immunity in patients with glioblastoma. PLoS One. 2012; 7 e31046 [PubMed: 22383993]
32. Rech AJ, Mick R, Martin S, Recio A, Aqui NA, Powell DJ Jr, Colligon TA, Trosko JA, Leinbach LI, Pletcher CH, Tweed CK, et al. CD25 blockade depletes and selectively reprograms regulatory T cells in concert with immunotherapy in cancer patients. Sci Transl Med. 2012; 4 134ra162
33. Attia P, Maker AV, Haworth LR, Rogers-Freezer L, Rosenberg SA. Inability of a fusion protein of IL-2 and diphtheria toxin (Denileukin Diftitox, DAB389IL-2, ONTAK) to eliminate regulatory T lymphocytes in patients with melanoma. J Immunother. 2005; 28: 582–592. [PubMed: 16224276]
34. Zamarin D, Hamid O, Nayak-Kapoor A, Sahebjam S, Sznol M, Collaku A, Fox FE, Marshall MA, Hong DS. Mogamulizumab in Combination with Durvalumab or Tremelimumab in Patients with Advanced Solid Tumors: A Phase I Study. Clin Cancer Res. 2020; 26: 4531–4541. [PubMed: 32586937]
35. Kurose K, Ohue Y, Wada H, Iida S, Ishida T, Kojima T, Doi T, Suzuki S, Isobe M, Funakoshi T, Kakimi K, et al. Phase Ia Study of FoxP3+ CD4 T_{reg} Depletion by Infusion of a Humanized Anti-CCR4 Antibody, KW-0761, in Cancer Patients. Clin Cancer Res. 2015; 21: 4327–4336. [PubMed: 26429981]
36. Kim JM, Rasmussen JP, Rudensky AY. Regulatory T cells prevent catastrophic autoimmunity throughout the lifespan of mice. Nat Immunol. 2007; 8: 191–197. [PubMed: 17136045]
37. Takahashi T, Kuniyasu Y, Toda M, Sakaguchi N, Itoh M, Iwata M, Shimizu J, Sakaguchi S. Immunologic self-tolerance maintained by CD25+CD4+ naturally anergic and suppressive T cells: induction of autoimmune disease by breaking their anergic/suppressive state. Int Immunol. 1998; 10: 1969–1980. [PubMed: 9885918]
38. Collison LW, Pillai MR, Chaturvedi V, Vignali DA. Regulatory T cell suppression is potentiated by target T cells in a cell contact, IL-35- and IL-10-dependent manner. J Immunol. 2009; 182: 6121–6128. [PubMed: 19414764]
39. Thornton AM, Shevach EM. CD4+CD25+ immunoregulatory T cells suppress polyclonal T cell activation in vitro by inhibiting interleukin 2 production. J Exp Med. 1998; 188: 287–296. [PubMed: 9670041]
40. Villarreal DO, L'Huillier A, Armington S, Mottershead C, Filippova EV, Coder BD, Petit RG, Princiotta MF. Targeting CCR8 Induces Protective Antitumor Immunity and Enhances Vaccine-Induced Responses in Colon Cancer. Cancer Res. 2018; 78: 5340–5348. [PubMed: 30026324]
41. Whiteside SK, Grant FM, Gyori DS, Conti AG, Imianowski CJ, Kuo P, Nasrallah R, Sadiyah F, Lira SA, Tacke F, Eil RL, et al. CCR8 marks highly suppressive T_{reg} cells within tumours but is dispensable for their accumulation and suppressive function. Immunology. 2021; 163: 512–520. [PubMed: 33838058]
42. Van Damme H, Dombrecht B, Kiss M, Roose H, Allen E, Van Overmeire E, Kancheva D, Martens L, Murgaski A, Bardet PMR, Blancke G, et al. Therapeutic depletion of CCR8(+) tumor-infiltrating regulatory T cells elicits antitumor immunity and synergizes with anti-PD-1 therapy. J Immunother Cancer. 2021; 9
43. Campbell JR, McDonald BR, Mesko PB, Siemers NO, Singh PB, Selby M, Sproul TW, Korman AJ, Vlach LM, Houser J, Sambanthamoorthy S, et al. Fc-Optimized Anti-CCR8 Antibody Depletes Regulatory T Cells in Human Tumor Models. Cancer Res. 2021; 81: 2983–2994. [PubMed: 33757978]
44. Alvisi G, Brummelman J, Puccio S, Mazza EM, Tomada EP, Losurdo A, Zanon V, Peano C, Colombo FS, Scarpa A, Alloisio M, et al. IRF4 instructs effector T_{reg} differentiation and immune suppression in human cancer. J Clin Invest. 2020; 130: 3137–3150. [PubMed: 32125291]

Europe PMC Funders Author Manuscripts

Europe PMC Funders Author Manuscripts

45. Mahata B, Pramanik J, van der Weyden L, Polanski K, Kar G, Riedel A, Chen X, Fonseca NA, Kundu K, Campos LS, Ryder E, et al. Tumors induce de novo steroid biosynthesis in T cells to evade immunity. Nat Commun. 2020; 11 3588 [PubMed: 32680985]
46. Groux H, O'Garra A, Bigler M, Rouleau M, Antonenko S, de Vries JE, Roncarolo MG. A CD4+ T-cell subset inhibits antigen-specific T-cell responses and prevents colitis. Nature. 1997; 389: 737–742. [PubMed: 9338786]
47. Roncarolo MG, Yssel H, Touraine JL, Betuel H, De Vries JE, Spits H. Autoreactive T cell clones specific for class I and class II HLA antigens isolated from a human chimera. J Exp Med. 1988; 167: 1523–1534. [PubMed: 3284961]
48. Gagliani N, Magnani CF, Huber S, Gianolini ME, Pala M, Licona-Limon P, Guo B, Herbert DR, Bulfone A, Trentini F, Di Serio C, et al. Coexpression of CD49b and LAG-3 identifies human and mouse T regulatory type 1 cells. Nat Med. 2013; 19: 739–746. [PubMed: 23624599]
49. Pedroza-Gonzalez A, Zhou G, Vargas-Mendez E, Boor PP, Mancham S, Verhoef C, Polak WG, Grunhagen D, Pan Q, Janssen H, Garcia-Romo GS, Biermann K, et al. Tumor-infiltrating plasmacytoid dendritic cells promote immunosuppression by Tr1 cells in human liver tumors. Oncoimmunology. 2015; 4 e1008355 [PubMed: 26155417]
50. Zhang P, Lee JS, Gartlan KH, Schuster IS, Comerford I, Varelias A, Ullah MA, Vuckovic S, Koyama M, Kuns RD, Locke KR, et al. Eomesodermin promotes the development of type 1 regulatory T (T(R)1) cells. Sci Immunol. 2017; 2
51. Gruarin P, Maglie S, De Simone M, Haringer B, Vasco C, Ranzani V, Bosotti R, Noddings JS, Larghi P, Facciotti F, Sarnicola ML, et al. Eomesodermin controls a unique differentiation program in human IL-10 and IFN-gamma coproducing regulatory T cells. Eur J Immunol. 2019; 49: 96–111. [PubMed: 30431161]
52. Bonnal RJP, Rossetti G, Lugli E, De Simone M, Gruarin P, Brummelman J, Drufuca L, Passaro M, Bason R, Gervasoni F, Della Chiara G, et al. Clonally expanded EOMES(+) Tr1-like cells in primary and metastatic tumors are associated with disease progression. Nat Immunol. 2021; 22: 735–745. [PubMed: 34017124]
53. Jin HT, Anderson AC, Tan WG, West EE, Ha SJ, Araki K, Freeman GJ, Kuchroo VK, Ahmed R. Cooperation of Tim-3 and PD-1 in CD8 T-cell exhaustion during chronic viral infection. Proc Natl Acad Sci U S A. 2010; 107: 14733–14738. [PubMed: 20679213]
54. Fiorentino DF, Bond MW, Mosmann TR. Two types of mouse T helper cell. IV. Th2 clones secrete a factor that inhibits cytokine production by Th1 clones. J Exp Med. 1989; 170: 2081–2095. [PubMed: 2531194]
55. Moore KW, de Waal Malefyt R, Coffman RL, O'Garra A. Interleukin-10 and the interleukin-10 receptor. Annu Rev Immunol. 2001; 19: 683–765. [PubMed: 11244051]
56. Tanikawa T, Wilke CM, Kryczek I, Chen GY, Kao J, Nunez G, Zou W. Interleukin-10 ablation promotes tumor development, growth, and metastasis. Cancer Res. 2012; 72: 420–429. [PubMed: 22123924]
57. Pastille E, Bardini K, Fleissner D, Adamczyk A, Frede A, Wadwa M, von Smolinski D, Kasper S, Sparwasser T, Gruber AD, Schuler M, et al. Transient ablation of regulatory T cells improves antitumor immunity in colitis-associated colon cancer. Cancer Res. 2014; 74: 4258–4269. [PubMed: 24906621]
58. Grant FM, Yang J, Nasrallah R, Clarke J, Sadiyah F, Whiteside SK, Imianowski CJ, Kuo P, Vardaka P, Todorov T, Zandhuis N, et al. BACH2 drives quiescence and maintenance of resting T_{reg} cells to promote homeostasis and cancer immunosuppression. J Exp Med. 2020; 217
59. Roychoudhuri R, Clever D, Li P, Wakabayashi Y, Quinn KM, Klebanoff CA, Ji Y, Sukumar M, Eil RL, Yu Z, Spolski R, et al. BACH2 regulates CD8(+) T cell differentiation by controlling access of AP-1 factors to enhancers. Nat Immunol. 2016; 17: 851–860. [PubMed: 27158840]
60. Igarashi K, Kurosaki T, Roychoudhuri R. BACH transcription factors in innate and adaptive immunity. Nat Rev Immunol. 2017; 17: 437–450. [PubMed: 28461702]
61. De Simone M, Arrigoni A, Rossetti G, Gruarin P, Ranzani V, Politano C, Bonnal RJP, Provasi E, Sarnicola ML, Panzeri I, Moro M, et al. Transcriptional Landscape of Human Tissue Lymphocytes Unveils Uniqueness of Tumor-Infiltrating T Regulatory Cells. Immunity. 2016; 45: 1135–1147. [PubMed: 27851914]

Europe PMC Funders Author Manuscripts

62. Plitas G, Konopacki C, Wu K, Bos PD, Morrow M, Putintseva EV, Chudakov DM, Rudensky AY. Regulatory T Cells Exhibit Distinct Features in Human Breast Cancer. Immunity. 2016; 45: 1122–1134. [PubMed: 27851913]

63. Kidani Y, Nogami W, Yasumizu Y, Kawashima A, Tanaka A, Sonoda Y, Tona Y, Nashiki K, Matsumoto R, Hagiwara M, Osaki M, et al. CCR8-targeted specific depletion of clonally expanded T_{reg} cells in tumor tissues evokes potent tumor immunity with long-lasting memory. Proc Natl Acad Sci U S A. 2022; 119

64. Bergmann C, Strauss L, Wang Y, Szczepanski MJ, Lang S, Johnson JT, Whiteside TL. T regulatory type 1 cells in squamous cell carcinoma of the head and neck: mechanisms of suppression and expansion in advanced disease. Clin Cancer Res. 2008; 14: 3706–3715. [PubMed: 18559587]

65. Scurr M, Ladell K, Besneux M, Christian A, Hockey T, Smart K, Bridgeman H, Hargest R, Phillips S, Davies M, Price D, et al. Highly prevalent colorectal cancer-infiltrating LAP(+) Foxp3(-) T cells exhibit more potent immunosuppressive activity than Foxp3(+) regulatory T cells. Mucosal Immunol. 2014; 7: 428–439. [PubMed: 24064667]

66. Marshall NA, Christie LE, Munro LR, Culligan DJ, Johnston PW, Barker RN, Vickers MA. Immunosuppressive regulatory T cells are abundant in the reactive lymphocytes of Hodgkin lymphoma. Blood. 2004; 103: 1755–1762. [PubMed: 14604957]

67. Yan H, Zhang P, Kong X, Hou X, Zhao L, Li T, Yuan X, Fu H. Primary Tr1 cells from metastatic melanoma eliminate tumor-promoting macrophages through granzyme B- and perforin-dependent mechanisms. Tumour Biol. 2017; 39 1010428317697554 [PubMed: 28378637]

68. Zappasodi R, Budhu S, Hellmann MD, Postow MA, Senbabaoglu Y, Manne S, Gasmi B, Liu C, Zhong H, Li Y, Huang AC, et al. Non-conventional Inhibitory CD4(+)Foxp3(-)PD-1(hi) T Cells as a Biomarker of Immune Checkpoint Blockade Activity. Cancer Cell. 2018; 33: 1017–1032. e1017 [PubMed: 29894689]

69. Eschweiler S, Clarke J, Ramirez-Suastegui C, Panwar B, Madrigal A, Chee SJ, Karydis I, Woo E, Alzetani A, Elsheikh S, Hanley CJ, et al. Intratumoral follicular regulatory T cells curtail anti-PD-1 treatment efficacy. Nat Immunol. 2021; 22: 1052–1063. [PubMed: 34168370]

70. Lahl K, Mayer CT, Bopp T, Huehn J, Loddenkemper C, Eberl G, Wirnsberger G, Dornmair K, Geffers R, Schmitt E, Buer J, et al. Nonfunctional regulatory T cells and defective control of Th2 cytokine production in natural scurfy mutant mice. J Immunol. 2009; 183: 5662–5672. [PubMed: 19812199]

71. Tian L, Altin JA, Makaroff LE, Franckaert D, Cook MC, Goodnow CC, Dooley J, Liston A. Foxp3(+) regulatory T cells exert asymmetric control over murine helper responses by inducing Th2 cell apoptosis. Blood. 2011; 118: 1845–1853. [PubMed: 21715314]

72. Freeman CM, Chiu BC, Stolberg VR, Hu J, Zeibecoglou K, Lukacs NW, Lira SA, Kunkel SL, Chensue SW. CCR8 is expressed by antigen-elicited, IL-10-producing CD4+CD25+ T cells, which regulate Th2-mediated granuloma formation in mice. J Immunol. 2005; 174: 1962–1970. [PubMed: 15699124]

73. Mikhak Z, Fukui M, Farsidjani A, Medoff BD, Tager AM, Luster AD. Contribution of CCR4 and CCR8 to antigen-specific T(H)2 cell trafficking in allergic pulmonary inflammation. J Allergy Clin Immunol. 2009; 123: 67–73. e63 [PubMed: 19062085]

74. McCully ML, Ladell K, Andrews R, Jones RE, Miners KL, Roger L, Baird DM, Cameron MJ, Jessop ZM, Whitaker IS, Davies EL, et al. CCR8 Expression Defines Tissue-Resident Memory T Cells in Human Skin. J Immunol. 2018; 200: 1639–1650. [PubMed: 29427415]

75. Guo Y, Xie YQ, Gao M, Zhao Y, Franco F, Wenes M, Siddiqui I, Bevilacqua A, Wang H, Yang H, Feng B, et al. Metabolic reprogramming of terminally exhausted CD8(+) T cells by IL-10 enhances anti-tumor immunity. Nat Immunol. 2021; 22: 746–756. [PubMed: 34031618]

76. Naing A, Infante JR, Papadopoulos KP, Chan IH, Shen C, Ratti NP, Rojo B, Autio KA, Wong DJ, Patel MR, Ott PA, et al. PEGylated IL-10 (Pegilodecakin) Induces Systemic Immune Activation, CD8(+) T Cell Invigoration and Polyclonal T Cell Expansion in Cancer Patients. Cancer Cell. 2018; 34: 775–791. e773 [PubMed: 30423297]

77. Tannir NM, Papadopoulos KP, Wong DJ, Aljumaily R, Hung A, Afable M, Kim JS, Ferry D, Drakaki A, Bendell J, Naing A. Pegilodecakin as monotherapy or in combination with anti-PD-1 or tyrosine kinase inhibitor in heavily pretreated patients with advanced renal cell carcinoma: Final

results of cohorts A, G, H and I of IVY Phase I study. Int J Cancer. 2021; 149: 403–408. [PubMed: 33709428]

78. Glisson BS, Leidner RS, Ferris RL, Powderly J, Rizvi NA, Keam B, Schneider R, Goel S, Ohr JP, Burton J, Zheng Y, et al. Safety and Clinical Activity of MEDI0562, a Humanized OX40 Agonist Monoclonal Antibody, in Adult Patients with Advanced Solid Tumors. Clin Cancer Res. 2020; 26: 5358–5367. [PubMed: 32816951]
79. Romano E, Kusio-Kobialka M, Foukas PG, Baumgaertner P, Meyer C, Ballabeni P, Michielin O, Weide B, Romero P, Speiser DE. Ipilimumab-dependent cell-mediated cytotoxicity of regulatory T cells ex vivo by nonclassical monocytes in melanoma patients. Proc Natl Acad Sci U S A. 2015; 112: 6140–6145. [PubMed: 25918390]
80. Arce Vargas F, Furness AJS, Litchfield K, Joshi K, Rosenthal R, Ghorani E, Solomon I, Lesko MH, Ruef N, Roddie C, Henry JY, et al. Fc Effector Function Contributes to the Activity of Human Anti-CTLA-4 Antibodies. Cancer Cell. 2018; 33: 649–663. e644 [PubMed: 29576375]
81. Freitas do Rosario AP, Lamb T, Spence P, Stephens R, Lang A, Roers A, Muller W, O'Garra A, Langhorne J. IL-27 promotes IL-10 production by effector Th1 CD4+ T cells: a critical mechanism for protection from severe immunopathology during malaria infection. J Immunol. 2012; 188: 1178–1190. [PubMed: 22205023]
82. Brummelman J, Mazza EMC, Alvisi G, Colombo FS, Grilli A, Mikulak J, Mavilio D, Alloisio M, Ferrari F, Lopci E, Novellis P, et al. High-dimensional single cell analysis identifies stem-like cytotoxic CD8(+) T cells infiltrating human tumors. J Exp Med. 2018; 215: 2520–2535. [PubMed: 30154266]
83. Brummelman J, Haftmann C, Nunez NG, Alvisi G, Mazza EMC, Becher B, Lugli E. Development, application and computational analysis of high-dimensional fluorescent antibody panels for single-cell flow cytometry. Nat Protoc. 2019; 14: 1946–1969. [PubMed: 31160786]
84. Collison LW, Vignali DA. In vitro T_{reg} suppression assays. Methods Mol Biol. 2011; 707: 21–37. [PubMed: 21287326]
85. Love MI, Huber W, Anders S. Moderated estimation of fold change and dispersion for RNA-seq data with DESeq2. Genome Biol. 2014; 15: 550. [PubMed: 25516281]

Europe PMC Funders Author Manuscripts

Europe PMC Funders Author Manuscripts

Europe PMC Funders Author Manuscripts

Europe PMC Funders Author Manuscripts

One sentence summary

CCR8^{+} T_{conv} cells undergo expansion and activation upon T_{reg} cell depletion and limit anti-tumor immunity through production of IL-10.

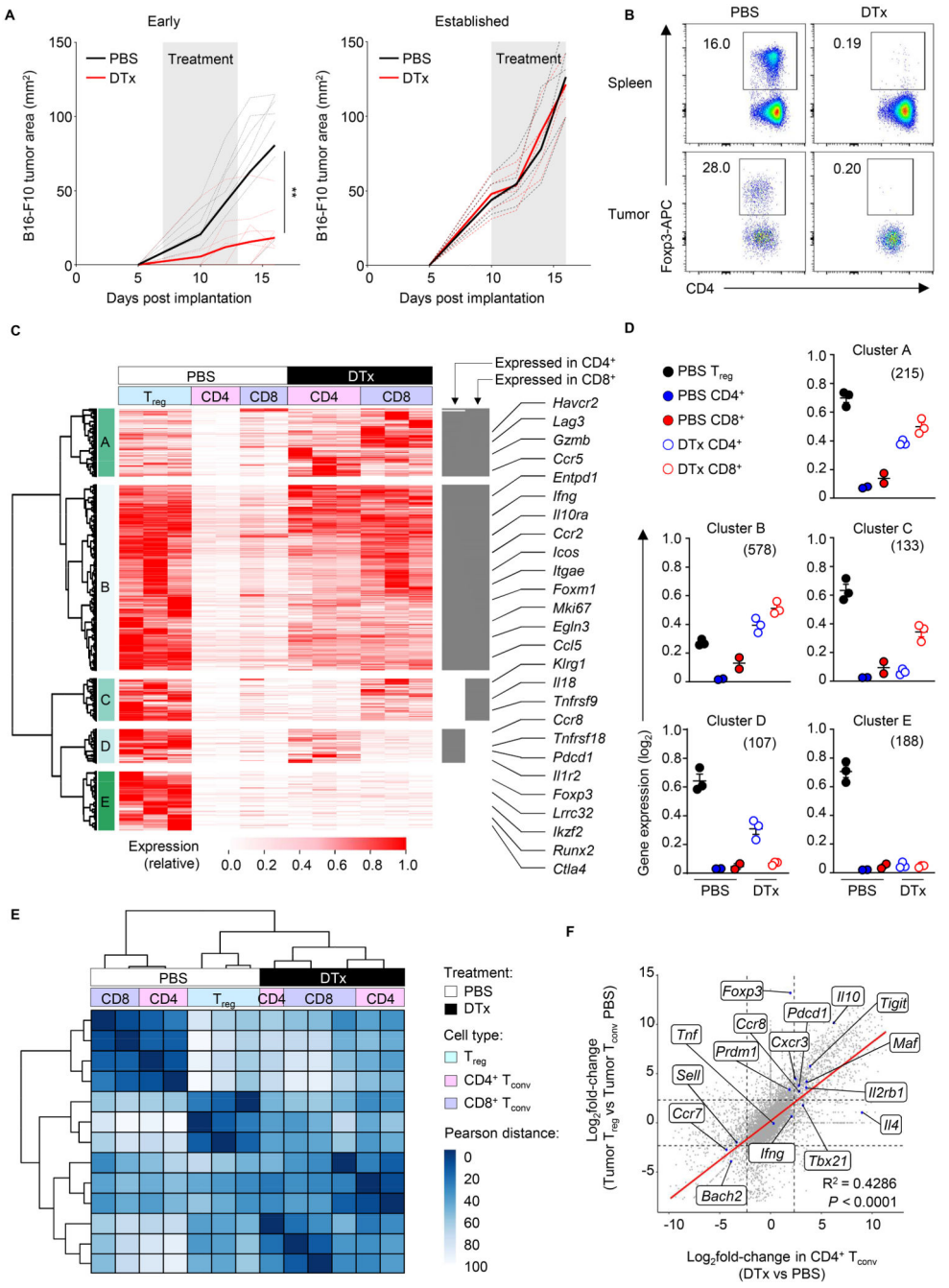


Figure 1. T_{reg} cell ablation causes T_{conv} cells to acquire transcriptional features of T_{reg} cells.

(**A**) Tumor growth of B16-F10 tumors subcutaneously implanted into *Foxp3*$^{EGFP\text{-}DTR}$ mice. Gray shading indicates time period over which PBS or DTx was administered (day 7-13 post-implantation, early disease; day 10-16 post-implantation, established). Dashed lines indicate individual mice. Solid line indicates average tumor area over time. Data representative of 4 individually repeated experiments, n > 5 $^{**}P < 0.01$; two-tailed Mann–Whitney *U*-test. (**B**) Representative frequency of Foxp3$^+$ T_{reg} cells among total CD4$^+$ T cells within spleens (top) or tumors (bottom) of *Foxp3*$^{EGFP\text{-}DTR}$ mice with established tumors

Europe PMC Funders Author Manuscripts
Europe PMC Funders Author Manuscripts

Europe PMC Funders Author Manuscripts

Europe PMC Funders Author Manuscripts

administered PBS or DTx. (**C**) Heatmap showing the relative expression of transcripts upregulated in intratumoral T_{reg} cells compared with $CD4^+$ T_{conv} cells (q<0.05; FC>4) in the indicated T cell subsets isolated at day 18 after implantation of B16-F10 tumors in *Foxp3*$^{EGFP\text{-}DTR}$ animals administered PBS or DTx. Colors indicate expression normalized to row maxima. x-axis hierarchical clustering of intratumoral T_{reg} cell-expressed transcripts identifies 5 clusters of genes with distinct expression patterns. Gray bars to right of heatmap indicate expression greater than a third of the expression of given transcripts in intratumoral T_{reg} cells. (**D**) Average expression of genes within the 5 clusters identified in each T cell subset. **(E)** Heatmap showing pairwise Pearson distances between the global gene expression profiles of the indicated T cell subsets from B16-F10 tumor-bearing *Foxp3*$^{EGFP\text{-}DTR}$ animals administered PBS or DTx. (**F**) Scatterplot comparing the global differences in gene expression between intratumoral T_{reg} cells and T_{conv} cells with transcriptional differences between $CD4^+$ T_{conv} cells isolated from DTx versus PBS-treated animals. A highly significant correlation is observed indicating transcriptional convergence of intratumoral T_{reg} cells with T_{conv} cells in absence of T_{reg} cells. Data from 2-4 biological replicates isolated on independent days (C-F).

Europe PMC Funders Author Manuscripts

Europe PMC Funders Author Manuscripts

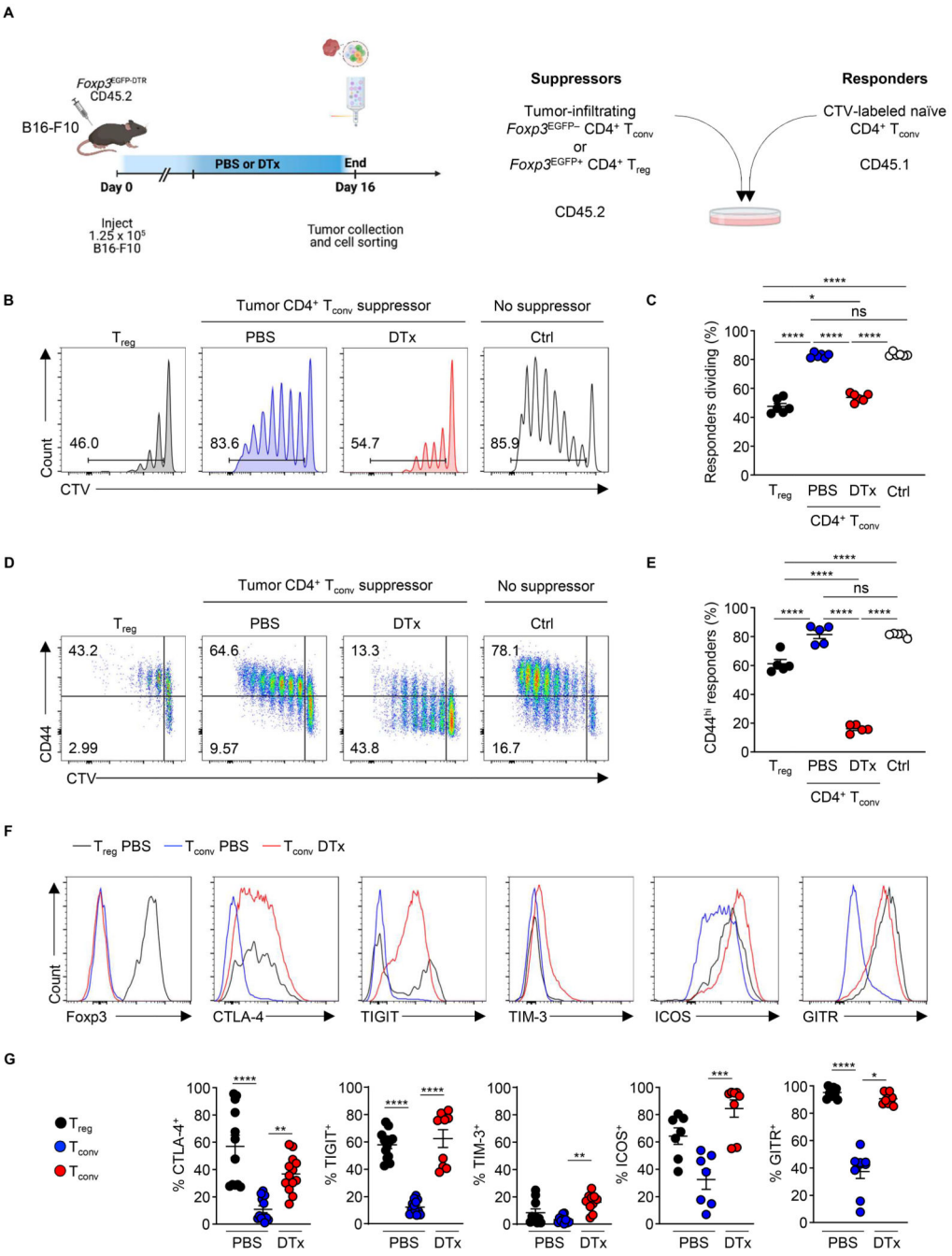


Figure 2. T_{reg} cell ablation promotes induction of suppressive function by $CD4^+$ T_{conv} cells.

(**A**) Experimental schema. B16-F10 cells were subcutaneously implanted into *Foxp3*$^{EGFP\text{-}DTR}$ $CD45.2^+$ mice and administered PBS or DTx on day 7, 9, 11, and 13. Cells were harvested from tumors of PBS- and DTx-treated animals at day 16 post-implantation and used in suppression assays. (**B** and **C**) *In vitro s*uppression assay. Proliferation of naïve $CD45.1^+$ $CD4^+$ T_{conv} responder (T_{resp}) cells 4 days cultured at a 4:1 ratio with indicated suppressor cell populations (*Foxp3*$^{EGFP-}$ T_{conv} cells from tumors of T_{reg}-replete (PBS) or T_{reg}-depleted (DTx) mice, or GFP^+ T_{reg} cells from tumors of T_{reg}-replete mice).

Europe PMC Funders Author Manuscripts

Europe PMC Funders Author Manuscripts

Representative histograms and replicate measurements of proliferation dye dilution at day 4 post-stimulation gated on CD45.1$^+$ T_{resp} cells shown. T_{resp} cell proliferation in the absence of a suppressor cell population was used as a control. Suppressor cells were co-cultured with responder T (Tresp) cells at a ratio of 1:4, with 2.5×10^4 suppressor CD4$^+$ T_{reg} or T_{conv} cells co-cultured with 1×10^5 Tresp cells in the presence of 5.0×10^4 antigen-presenting cells (APC). Data are representative of > 4 independently repeated experiments, n > 5 per group; ordinary one-way ANOVA, Tukey's multiple comparisons. (**D** and **E**) Representative histograms and replicate measurements of CD44 expression by CD45.1$^+$ T_{resp} cells incubated with indicated suppressor cell populations. (**F-G**) Representative flow cytometry and replicate measurements of the expression of the indicated proteins by intratumoral T_{reg} cells and CD4$^+$ T_{conv} cells isolated at day 16 after implantation of B16-F10 tumors in *Foxp3*$^{EGFP\text{-}DTR}$ mice treated with PBS or DTx. Data are representative of > 3 independently repeated experiments, n > 7 per group. ****P <0.0001; ns, not significant; one-way ANOVA Kruskal-Wallis, Dunn's multiple comparisons test. Error bars show standard error of the mean (s.e.m.)

Europe PMC Funders Author Manuscripts

Europe PMC Funders Author Manuscripts

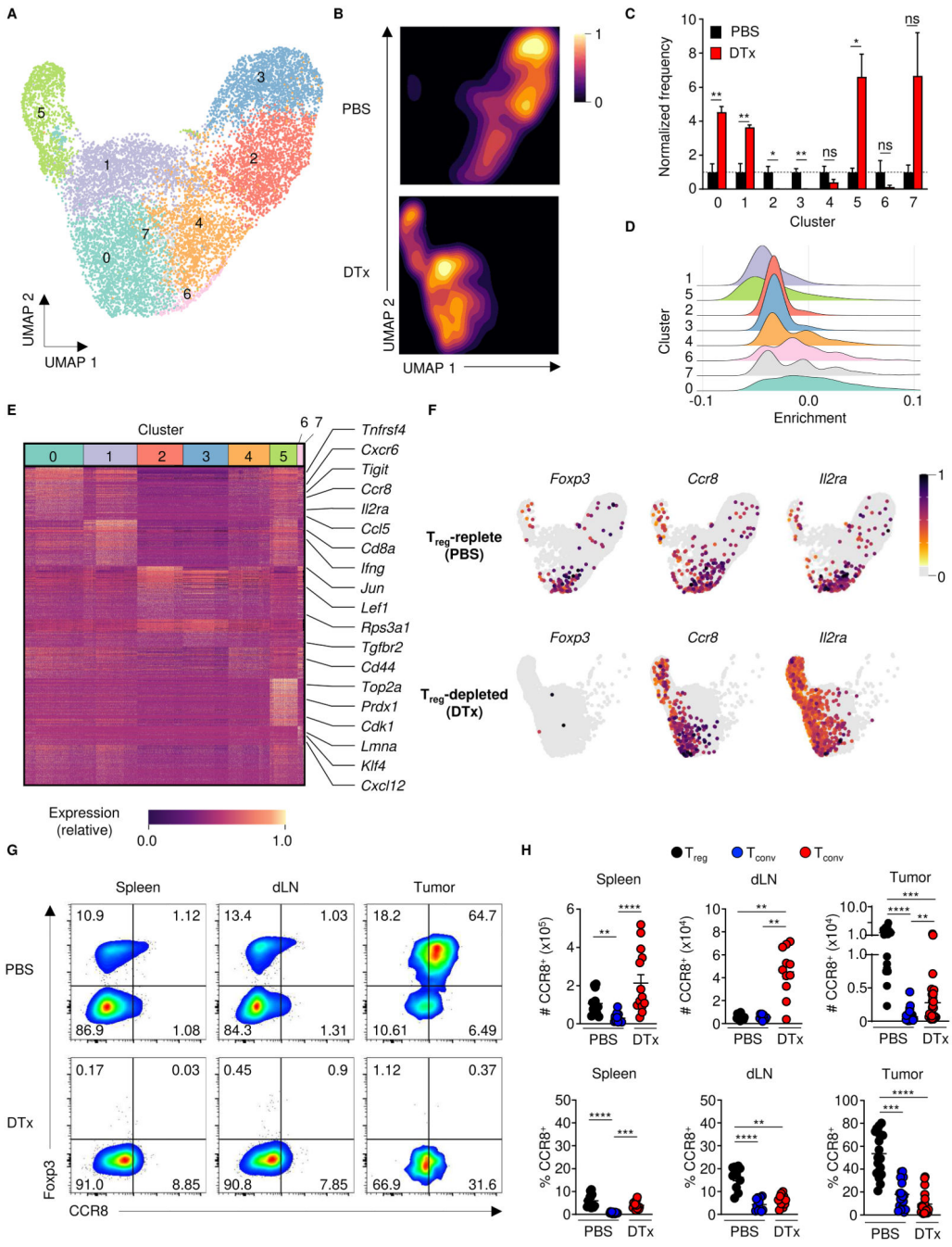


Figure 3. T_{reg} cell ablation promotes the expansion of tumor-infiltrating CCR8$^+$ T_{conv} cells.

(**A**) Uniform manifold approximation and projection (UMAP) of scRNA-Seq of TCRβ$^+$ cells isolated at day 16 after implantation of B16-F10 tumors in *Foxp3*$^{EGFP\text{-}DTR}$ mice treated with PBS or DTx on days 7, 9, 11 and 13. (**B**) Density plots showing change in distribution of cells within tumors of T_{reg}-replete (PBS) and T_{reg}-depleted (DTx) animals. (**C**) Relative frequency of cells within each cluster normalized to their average ratio among PBS animals. N = 3 biological replicates per group. (**D**) Average enrichment of expression of the genes in Cluster D from Fig. 1C across scRNA-Seq clusters, (n=3,

unpaired two-tailed Student's *t*-test, $*P < 0.05$, $**P < 0.01$). (**E**) Heatmap showing the expression of differentially upregulated genes in each cluster identified. (**F**) UMAP plots showing expression of indicated genes within T cells of tumors from tumor-bearing PBS- or DTx-treated *Foxp3*$^{EGFP\text{-}DTR}$ animals. (**G**) Representative flow cytometry and (**H**) replicate measurements of total counts (top) and the frequency (bottom) of CCR8^{+} of CD4^{+} T_{conv} cells from spleens, draining lymph nodes (dLN) and tumors of B16-F10 tumor-bearing *Foxp3*$^{EGFP\text{-}DTR}$ mice treated with PBS or DTx. Data are representative of 3 independently repeated experiments (**G** and **H**). Numbers in gates show percentages. n > 10. one-way ANOVA Kruskal-Wallis, Dunn's multiple comparisons test. $**P<0.01$, $***P < 0.001$, $****P < 0.0001$; Error bars show standard error of the mean (s.e.m.)

Europe PMC Funders Author Manuscripts

Europe PMC Funders Author Manuscripts

Europe PMC Funders Author Manuscripts

Europe PMC Funders Author Manuscripts

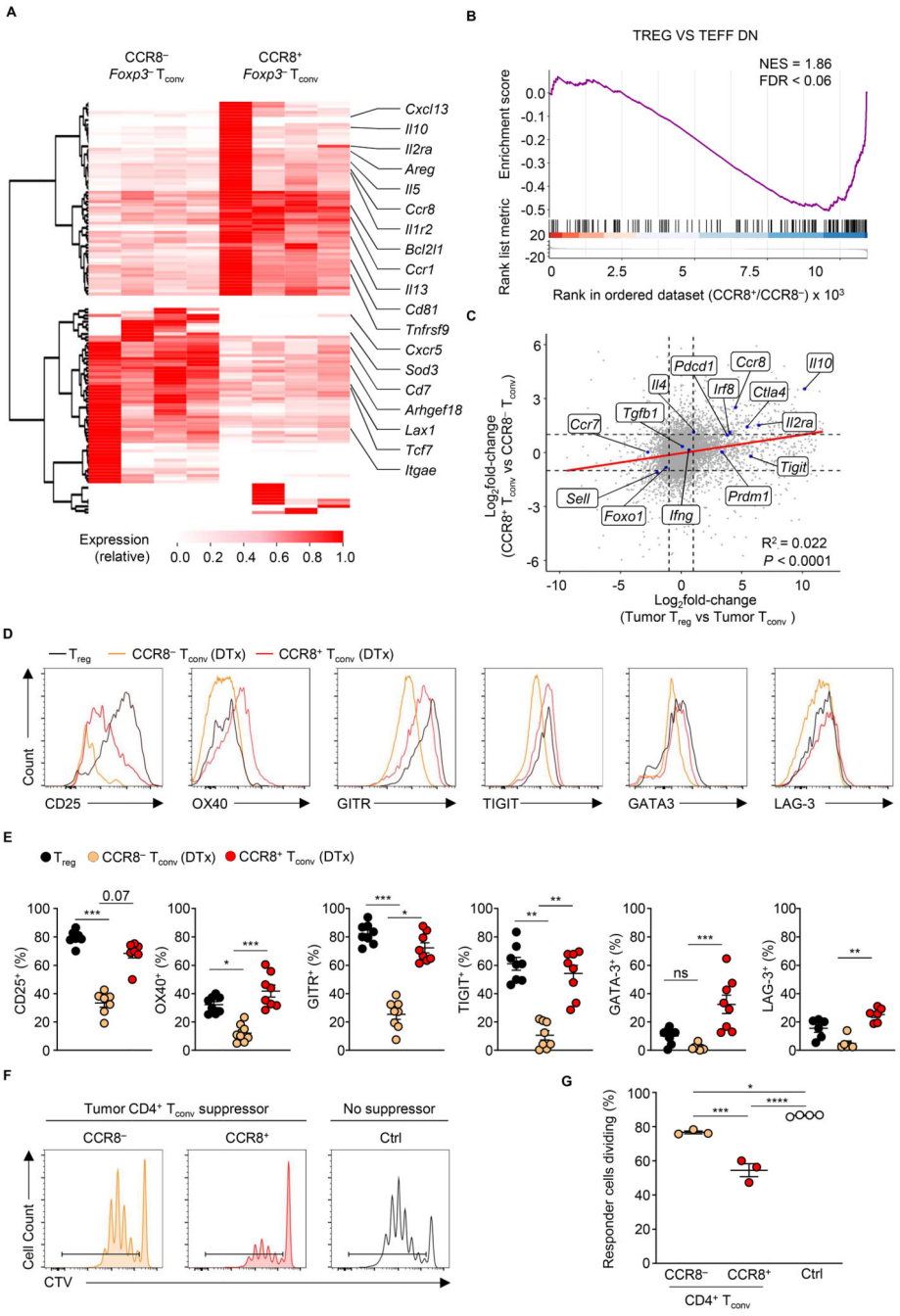


Figure 4. CCR8 marks highly suppressive T_{conv} cells.

(**A**) Heatmap showing the relative expression of differentially expressed genes between intratumoral CCR8$^+$ and CCR8$^-$ CD4$^+$ T_{conv} cells (q<0.05; |FC|>3) isolated at day 16 after subcutaneous implantation of B16-F10 tumors of T_{reg}-depleted *Foxp3*$^{EGFP\text{-}DTR}$ animals treated with DTx at days 7, 9, 11 and 13. Data from 4 biological replicates isolated on the same day. (**B**) Gene-set enrichment analysis (GSEA) demonstrating a negative enrichment of genes upregulated in *Foxp3*$^-$ T_{conv} cells *vs* *Foxp3*$^+$ T_{reg} cells among CCR8$^+$ T_{conv} cells compared with CCR8$^-$ T_{conv} cells isolated from tumors of DTx-treated *Foxp3*$^{EGFP\text{-}DTR}$

Europe PMC Funders Author Manuscripts

Europe PMC Funders Author Manuscripts

mice. (**C**) Scatterplot comparing global changes in gene expression between intratumoral T_{reg} and T_{conv} cells with transcriptional differences between $CCR8^+$ and $CCR8^-$ $CD4^+$ T_{conv} cells. (**D**) Representative flow cytometry and (**E**) replicate measurements of the expression of the indicated proteins from intratumoral T_{reg} cells and $CCR8^+$ and $CCR8^-$ $CD4^+$ T_{conv} cells from tumors of B16-F10 tumor-bearing *Foxp3*$^{EGFP\text{-}DTR}$ mice treated with PBS or DTx. Data are representative of 3 independently repeated experiments n > 4 one-way ANOVA Kruskal-Wallis, Dunn's multiple comparisons test. *$P < 0.05$, **$P < 0.01$, ***$P < 0.001$, ****$P < 0.0001$, ns, not significant. (**F**) Representative histograms and (**G**) replicate measurements of T_{resp} cells (naïve $CD45.1^+$ $CD4^+$ T_{conv} cells) incubated with intratumoral $CD45.2^+$ $TCR\beta^+$ $CD4^+$ GFP^- $CCR8^-$ or $CD45.2^+$ $TCR\beta^+$ $CD4^+$ GFP^- $CCR8^+$ suppressor T_{conv} cells isolated at day 16 after implantation of B16-F10 tumors in *Foxp3*$^{EGFP\text{-}DTR}$ mice. Suppressor cells were incubated with responders at a ratio of 1:8, with 1.25×10^4 suppressor $CD4^+$ T_{conv} cells co-cultured with 1×10^5 Tresp cells in the presence of 5×10^4 APC. Cell proliferation of T_{resp} cells was analyzed after 4 days. Data are representative of 2 independently repeated experiments n > 3. ordinary one-way ANOVA, Tukey's multiple comparisons. *$P < 0.05$; ***$P < 0.001$, ****$P < 0.0001$; Error bars show standard error of the mean (s.e.m.)

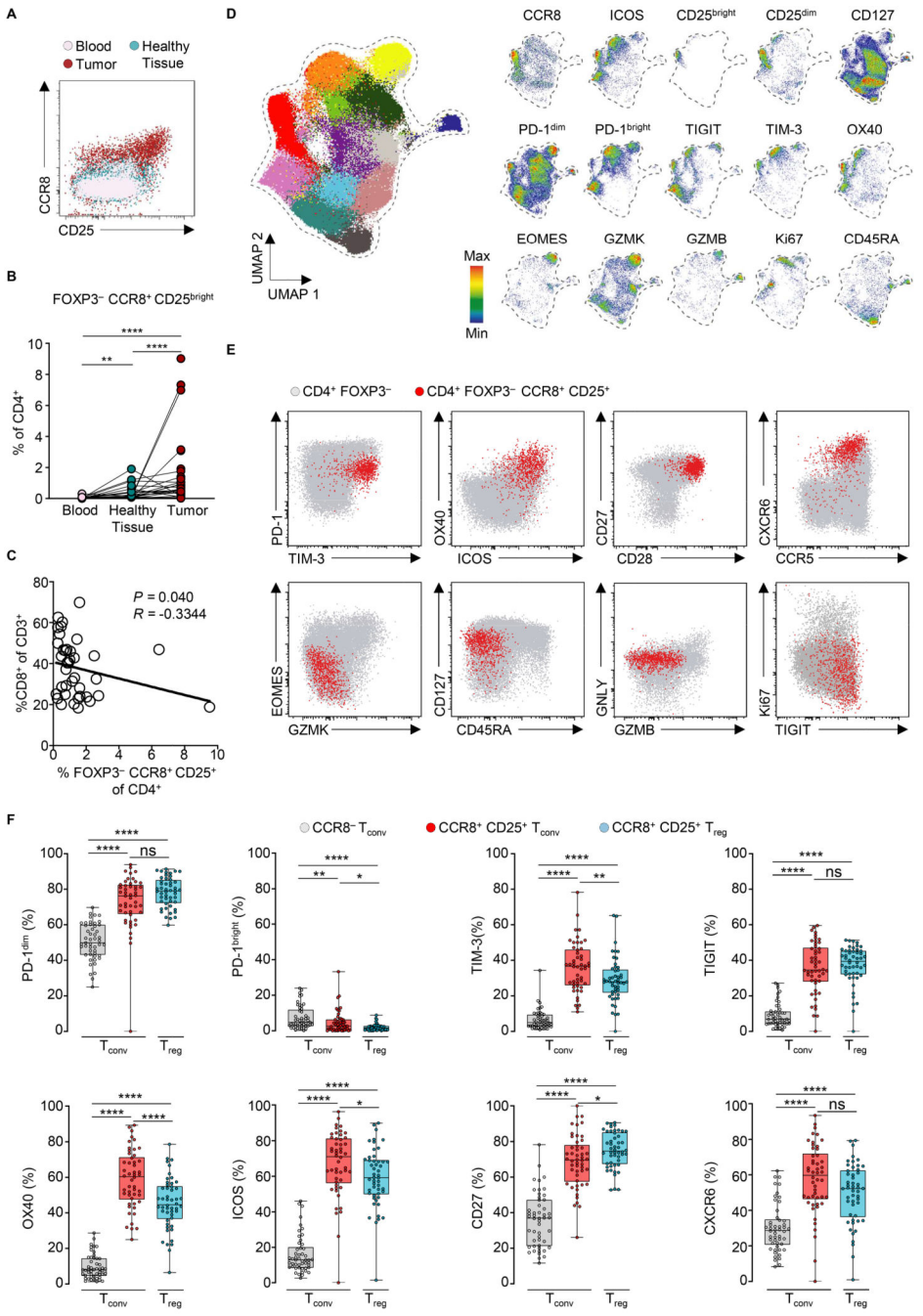


Figure 5. CCR8$^+$ T$_{conv}$ cells expressing high levels of CD25 are found within the tumors of NSCLC patients.

(**A**) CCR8 and CD25 expression among FOXP3$^-$ CD4$^+$ T cells from representative samples from NSCLC patients (n=48). (**B**) Frequency of FOXP3$^-$ CCR8$^+$ CD25^{bright} cells among CD4$^+$ T cells from the indicated patients' samples. Lines indicate paired samples. (**C**) Correlation of the frequency of CD8$^+$ T cells (of CD3$^+$ T cells) with FOXP3$^-$ CCR8$^+$ CD25^{bright} cells (of CD4$^+$ T cells) in tumors from patient samples. (**D**) UMAP analysis of concatenated CD4$^+$ FOXP3$^-$ T$_{conv}$ cells. Colors depict cell clusters identified by Phenograph

Europe PMC Funders Author Manuscripts
Europe PMC Funders Author Manuscripts

(k=500). Separate UMAP plots of relative marker expression by concatenated $CD4^+$ T cells from tumors. (**E**) Representative frequency and (**F**) replicate measurements of indicated markers from patient samples, box plots show median and interquartile range (IQR). Bars indicate standard deviation. Dots depict values of a single tumor sample. $^{**}P < 0.01$, $^{***}P < 0.001$, $^{****}P < 0.0001$; two-tailed Mann–Whitney *U*-test.

Europe PMC Funders Author Manuscripts

Europe PMC Funders Author Manuscripts

Europe PMC Funders Author Manuscripts

Europe PMC Funders Author Manuscripts

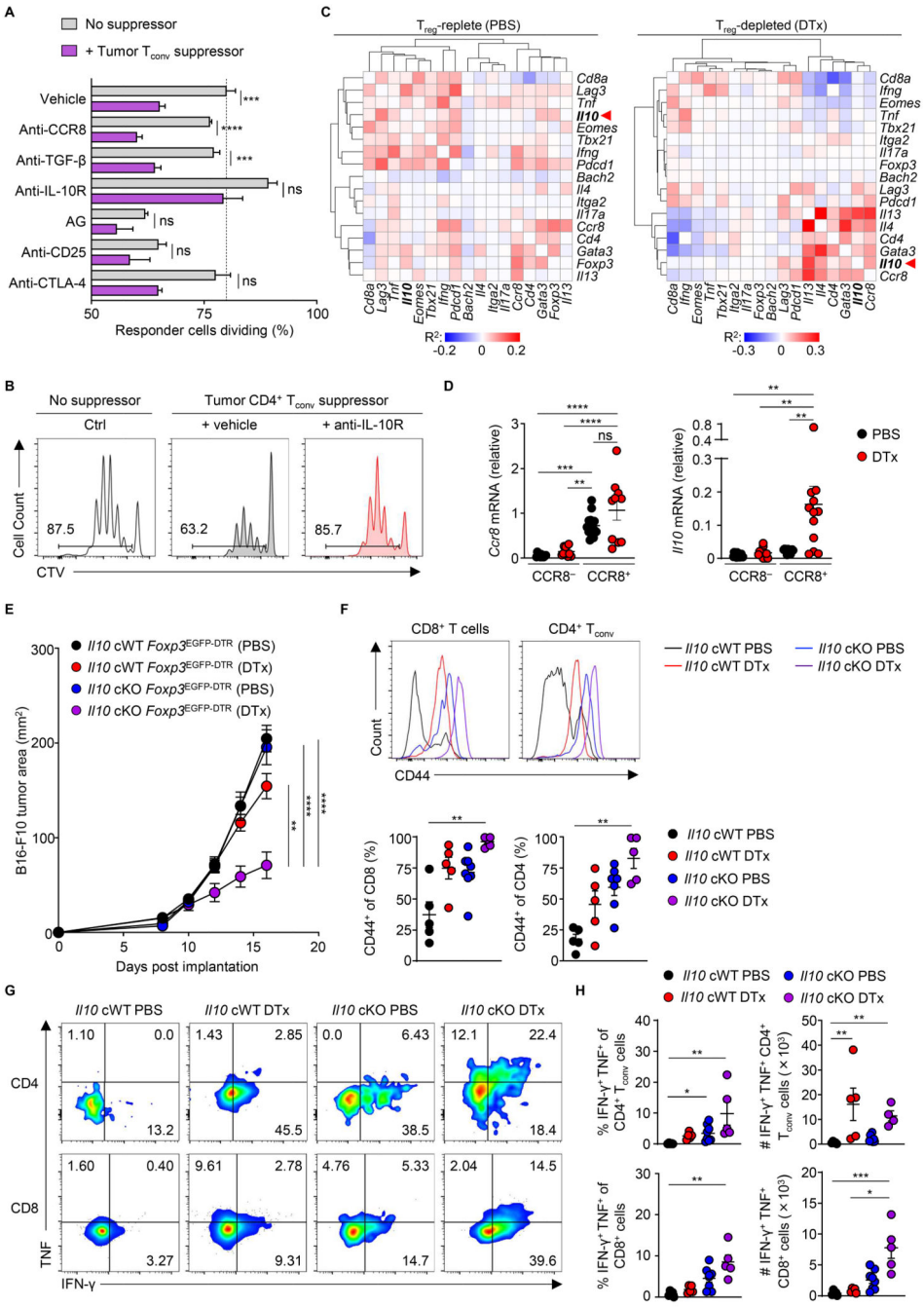


Figure 6. IL-10 production by CD4$^+$ T_{conv} cells limits anti-tumor immunity upon T_{reg} cell depletion.

(**A**) Screen to identify mechanisms of suppression by CD4$^+$ T_{conv} cells from tumors of T_{reg}-depleted animals. Proliferation of CTV-labeled naïve splenic CD4$^+$ T_{conv} responder cells (T_{resp}) cultured alone or at a ratio of 8:1 with CD4$^+$ *Foxp3*$^{EGFP-}$ T_{conv} suppressor cells (T_{supp}) isolated at day 16 from B16-F10 tumors of DTx-treated *Foxp3*$^{EGFP-DTR}$ animals. Cells were cultured alone (gray) or with suppressors (purple) and with indicated reagents. AG, aminoglutethimide. CD45.2$^+$ GFP$^-$ T_{conv} suppressor cells were co-cultured

Europe PMC Funders Author Manuscripts

Europe PMC Funders Author Manuscripts

with 1.25×10^4 suppressor $CD4^+$ T_{conv} cells in the presence of 5.0×10^4 antigen-presenting cells (APC). Data are representative of 2 independently repeated experiments n > 3. *P* values show significance of difference between no suppressor and suppressor (Student *t* test) and are Bonferroni corrected. (**B**) Representative frequency of dividing T_{resp} cells incubated with tumor $CD4^+$ GFP^- T_{conv} cells in the presence of anti-IL-10R antibodies or vehicle. T_{resp} cells without tumor T_{conv} cells were used as a control. (**C**) Co-correlation between the expression of indicated genes within single cell gene expression profiles of T cells from tumors of PBS- or DTx-treated B16 tumor-bearing *Foxp3*$^{EGFP\text{-}DTR}$ animals. Pearson correlation co-efficient values are indicated by color scale and genes are hierarchically clustered to identify clusters of co-expressed transcripts within T cell populations. scRNA-Seq data are representative of 3 biological replicates per group. (**D)** Measurement of *Ccr8* and *Il10* mRNA expression within $CCR8^-$ and $CCR8^+$ T_{conv} cells from PBS- and DTx-treated animals. Data representative of 3-4 biological replicates per group. ordinary one-way ANOVA, Tukey's multiple comparisons. ns, not significant. (**E**) Tumor area of heterotopic B16-F10 melanoma tumors at indicated time-points following implantation into *Il10*$^{flox/flox}$ *Cd4*^{Cre} *Foxp3*$^{EGFP\text{-}DTR}$ or *Il10*$^{+/+}$ *Cd4*^{Cre} *Foxp3*$^{EGFP\text{-}DTR}$ control mice administered DTx or PBS from day 10-16 post-implantation. Data are representative of 2 independently repeated experiments, n > 7. ordinary one-way ANOVA, Tukey's multiple comparisons. (**F**) Representative histograms (top) and replicate measurements (bottom) of the frequency of $CD8^+$ $CD44^+$ T cells and $Foxp3^-$ $CD4^+$ $CD44^+$ T_{conv} cells from tumors of animals within indicated treatment groups. (**G**) Representative frequency and (**H**) replicate measurements of the frequency (top) and total counts (bottom) of $CD8^+$ IFN-γ^+ TNF^+ T cells within tumors. Data are representative of 2 independently repeated experiments, n > 4, one-way ANOVA, Kruskal-Wallis, Dunn's multiple comparisons test. $*P < 0.05$; $**P < 0.01$; $***P < 0.001$, $****P < 0.0001$. Error bars show standard error of the mean (s.e.m.)

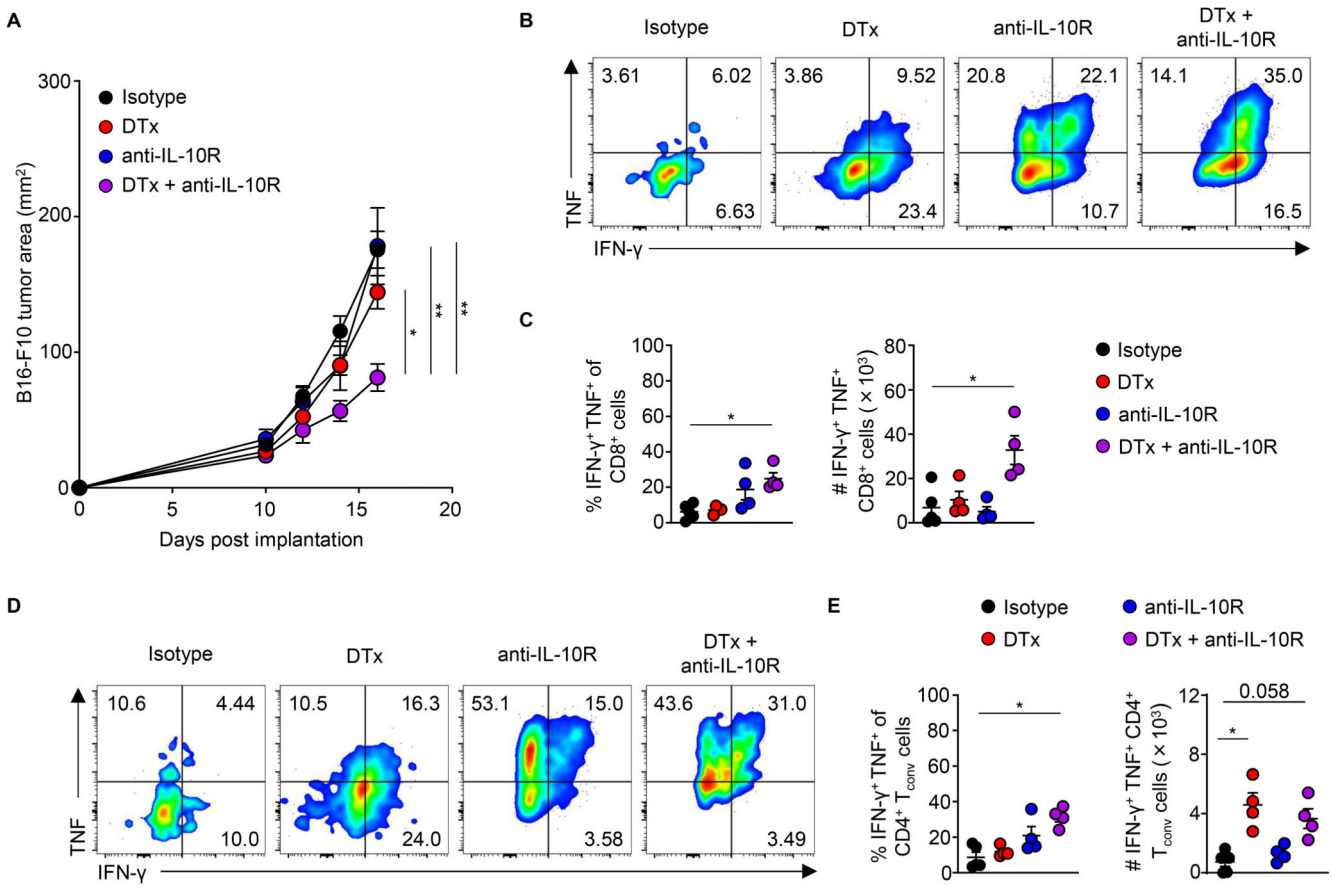


Figure 7. Blockade of IL-10 signaling synergizes with T_{reg} cell-depletion to drive potent anti-tumor immune responses.

(**A**) Tumor area of B16-F10 melanoma tumors at indicated time-points following implantation into *Foxp3*$^{EGFP\text{-}DTR}$ animals administered indicated combinations of DTx and anti-IL-10R or control reagents from days 10-16 after tumor implantation. Data are representative of 2 independently repeated experiments. n > 10, ordinary one-way ANOVA, Tukey's multiple comparisons. *$P < 0.05$ **$P < 0.01$; (**B**) Representative frequency and (**C**) replicate measurements of the frequency and total counts of CD8$^+$ IFN-γ^+ TNF$^+$ T cells from tumors. n > 3, one-way ANOVA, Kruskal-Wallis, Dunn's multiple comparisons test., *$P < 0.05$. (**D**) Representative frequency and (**E**) replicate measurements of the frequency and total counts of Foxp3$^-$ CD4$^+$ IFN-γ^+ TNF$^+$ T cells from tumors. Data from > 2 independent biological replicates. n > 3, Kruskal-Wallis, Dunn's multiple comparisons test., *$P < 0.05$; Error bars show standard error of the mean (s.e.m.)

Europe PMC Funders Author Manuscripts
Europe PMC Funders Author Manuscripts